Screening and functional prediction of differentially expressed circular RNAs in human glioma of different grades

Xiuchao Geng[1,2,*], Yuhao Zhang[3,4,*], Qiang Li[5,*], Wang Xi[6], Wentao Yu[5], Liang Shi[7], Xiaomeng Lin[8], Shaoguang Sun[9], Hong Wang[1,2,3]

[1]Faculty of Integrated Traditional Chinese and Western Medicine, Hebei University of Chinese Medicine, Shijiazhuang 050091, PR China
[2]Hebei Key Laboratory of Chinese Medicine Research on Cardio-cerebrovascular Disease, Hebei University of Chinese Medicine, Shijiazhuang 050091, PR China
[3]School of Clinical Medicine, Hebei University, Baoding 071000, PR China
[4]Department of Neurosurgery, Affiliated Hospital of Hebei University, Baoding 071000, PR China
[5]Faculty of Acupuncture-Moxibustion and Tuina, Hebei University of Chinese Medicine, Shijiazhuang 050200, PR China
[6]Department of Neurosurgery, The Second Hospital of Hebei Medical University, Shijiazhuang 050000, PR China
[7]Endoscope Room, Department of General Surgery, Cangzhou Central Hospital, Cangzhou 061001, PR China
[8]Departments of Breast Surgery, Affiliated Hospital of Hebei University, Baoding 071000, PR China
[9]Department of Biochemistry and Molecular Biology, Key Laboratory of Medical Biotechnology of Hebei Province, Hebei Medical University, Shijiazhuang 050017, PR China
*Equal contribution

Correspondence to: Hong Wang, Shaoguang Sun; **email:** bossw@vip.sina.com, https://orcid.org/0000-0001-6905-438X; sunshaoguang00@163.com, https://orcid.org/0000-0002-2827-0948

ABSTRACT

Circular RNAs (circRNAs) have a critical regulatory function in human glioma. However, novel circRNAs related to different pathological grades of glioma and their crucial potential function are worth screening and prediction. CircRNA expression profiling was performed for 6 paired high- and low-grade glioma tissues and 5 adjacent normal brain tissues through next-generation sequencing. Quantitative real-time PCR (qRT-PCR) was conducted to validate circRNA expression. Bioinformatics analysis was performed, and circRNA-miRNA-mRNA networks were constructed. The expression and survival data of miRNAs and target genes were examined by GEPIA, Chinese Glioma Genome Atlas (CGGA), ONCOMINE, and cBioPortal databases. The RNA binding proteins (RBPs), open reading frames (ORFs) and N6-methyladenosine (m6A) modifications of the identified circRNAs were also predicted. Through multilevel research screening, 4 circRNAs (hsa_circ_0000915, hsa_circ_0127664, hsa_circ_0008362, and hsa_circ_0001467) were associated with glioma of different pathological grades and could be preferred candidates for subsequent functional analysis. Therefore, circRNAs are associated with the different pathological grades of glioma and reveal their potential critical regulatory function. CircRNAs might provide vital molecular biomarkers and potential therapeutic targets for glioma.

INTRODUCTION

As a commonly seen human intracranial tumor, glioma can be further classified into high-grade (WHO III-IV) and low-grade (WHO I-II) tumors based on histopathological evaluation conducted by the WHO [1]. High-grade glioma (HGG), particularly glioblastoma (GBM) (grade IV), is the most lethal primary brain tumor

because of its highly infiltrative growth characteristics. Low-grade gliomas (LGGs), such as diffuse astrocytic and oligodendroglial tumors, have low-grade malignancy and slow growth rates, resulting in a long survival time for patients. There are also several reports of progression of some LGG into HGG in the clinic [2]. However, which factors influence glioma grade is unclear, and the mechanisms underlying the progression, etiology, pathogenesis and molecular characteristics of the different grades of glioma require further study.

As a novel kind of endogenous noncoding RNA (ncRNA), circular RNAs (circRNAs) possess a covalently closed structure with the absence of a 5′ and 3′ end [3]. CircRNAs are specifically expressed in cells or tissues, evolutionarily conserved across species, and relatively stable as a result of resistance to RNase R [4]. CircRNAs have been associated with how malignant tumors are regulated, including gliomas, as indicated by the latest studies. CircRNAs have crucial functions in regulating the cell cycle, apoptosis, angiogenesis, proliferation, invasion, migration, metastasis and radio- and chemoresistance in glioma cells [5–7]. Recent reports have claimed that certain circRNAs are closely related to the pathological grade of gliomas. For example, circFOXO3 [8], circNT5E [9], and hsa_circ_0001730 [10] are differentially expressed in HGG and LGG. CircRNA expression is disordered in HGG compared with matching normal tissues or cells [11]. Currently, as a detection method, next-generation sequencing is a crucial method to explore novel circRNAs. However, the differentially expressed circRNAs of different grades of human glioma have not been fully investigated. Novel circRNAs related to different pathological grades of glioma and their specific crucial functions are worth screening and prediction.

The biological function of circRNAs is mainly reflected in the regulation of gene expression at the transcriptional or posttranscriptional level. Regarding their regulatory mechanisms, circRNAs have been confirmed to act as miRNA sponges to regulate the expression of miRNA target genes by competitively binding miRNA response elements (MREs). Acting as a miRNA sponge or as a competing endogenous RNA (ceRNA) is still one of the most recognized mechanisms. CircRNAs could compete with mRNAs, lncRNAs, and pseudogenes that also contain MREs to adsorb miRNAs, relieve the negative regulation of miRNAs on target gene expression, and improve the function and expression levels of target genes. For instance, circCCDC9 could act as a miR-6792-3p sponge to relieve the negative regulation of miR-6792-3p on its target gene *CAV1* and then inhibit the

progression of gastric cancer [12]. CircMAPK4 could function as an oncogene and suppress apoptosis in glioma by sponging miR-125a-3p [13]. Therefore, to explore more circRNAs closely related to multiple cancers, including glioma, the mechanism of miRNA sponges is still a direction worthy of attention and research.

Apart from their function as miRNA sponges, circRNAs can also function as RBP sponges or protein scaffolds and can be translated into either peptides or proteins [14]. According to one report, an internal ribosome entry site (IRES)-driven open reading frame (ORF) is present in circ-SHPRH, which has been reported to be translated into SHPRH-146aa [15]. This finding suggests that the potential translation function may be an important research direction for circRNAs. N6-methyladenine (m^6A) modification is the most abundant form of posttranscriptional RNA modification in eukaryotes. In recent years, the role of m^6A in cancers including gliomas has been gradually recognized [16, 17]. It has been reported that N6-methyladenosine (m^6A) modification could also initiate the translation of circRNAs [18]. In linear mRNAs, m^6A is usually located around the start and stop codons, and it also appears to be enriched in the junction sequences of circRNAs [19]. Recently, it has been newly reported that m^6A can also mediate the biogenesis of coding circRNAs [20], and circRNA can not only be modified by m^6A but also regulate the process of m^6A modification by binding to the enzyme modified by m^6A [21]. However, these potential vital functions of circRNAs have not been fully investigated and clarified. Hence, the prediction and analysis of RBP sponges and m^6A modification of circRNAs requires deep future research.

In this research, we innovatively performed RNA-seq analysis of gliomas of different grades and analyzed and predicted the multiple crucial functions of the identified circRNAs. Our results demonstrated that 4 differentially expressed circRNAs are associated with the pathological characteristics of glioma, and their multilevel functions merit systematic analysis. The potential utility of circRNAs as vital molecular biomarkers or potential therapeutic targets in glioma has been indicated.

RESULTS

CircRNA expression profiles

CircRNA expression profiles were performed on 6 HGG and 6 LGG patient tissues as well as 5 adjacent normal tissues. After the raw data were quantile normalized, the circRNA expression profiles were

observed. A fold change (FC) > 2 and p < 0.05 were the cutoff criteria to identify differentially expressed circRNAs between each pair of groups. Eventually, a total of 153799 circRNAs were discovered in the high-low grade group. Among them, 296 exhibited upregulation and 332 showed downregulation. With regard to the high-normal grade group, 118649 circRNAs were found. Among them, 718 showed upregulation, and 269 exhibited downregulation. For the low-normal grade group, 128334 circRNAs were discovered, among which 945 showed upregulation and 252 exhibited downregulation (Figure 1A). As demonstrated by the hierarchical clustering heatmap (Figure 1B), a distinctive mode of circRNA expression was observed among the three groups. Based on how the different circRNA types were distributed, a large proportion of the circRNAs originate from exons. In comparison, other circRNAs stem from intronic and/or intergenic genomic regions (Figure 1C). How the expression of circRNAs was differentiated to a significant extent between each group is presented in the form of volcano plots (Figure 2A). The Circos plots show all the differentially expressed circRNAs compared with HGG, LGG tissue and adjacent normal brain tissue (Figure 2B), which led to the finding that every single chromosome showed differences in the expression of circRNAs.

Validation of the circRNA-seq data via qRT-PCR

To verify the circRNA-seq analysis data, we focused on the downregulated circRNAs with certain circBase IDs. Five circRNAs were first selected as examples in further analysis from the most downregulated circRNAs. A design was developed for the divergent primers spanning the back-splice junction sites. The qRT-PCR-amplified products of each candidate circRNA were identified by Sanger sequencing to validate the sequence of head-to-tail splice junctions. The primer sequences are presented in Supplementary Table 1.

Samples were obtained from 15 HGG tissues, 15 LGG tissues, and 15 adjacent normal tissues for qRT-PCR analysis. The analysis revealed that 4 circRNAs were significantly downregulated, showing the same trend as the RNA-seq results, except 1 circRNA (hsa_circ_0000199) was not significantly differentially expressed. In conclusion, the qRT-PCR results suggested that the RNA-seq was reliable and that most of the screened circRNAs merit further investigation. As shown in Figure 3A, the expression of hsa_circ_0000915 and hsa_circ_0127664 was downregulated in the HGG group compared with the LGG group, and the expression of hsa_circ_0001467 and hsa_circ_0008362 was downregulated in the HGG group compared with the normal group (Figure 3B).

Sanger sequencing was used to validate the head-to-tail splice junctions of the above 4 circRNAs (Figure 3C). Through characterization of the identified circRNAs, we found that hsa_circ_0000915 (position: chr19: 18650181-18650530) is encoded from exons 3 and 4 of *FKBP8*. Its splicing length is 259 bp. Moreover, the characterization information for hsa_circ_0000915, hsa_circ_0127664, hsa_circ_0008362, and hsa_circ_0001467 were drawn via circPrimer software [22] (Figure 3D).

Diagnostic accuracy analysis of candidate circRNAs

To explore the potential diagnostic value of the identified circRNAs, receiver operating characteristic (ROC) curves were analyzed. Relative to low grade, HGG patients showed a downregulation of hsa_circ_0000915 and hsa_circ_0127664 expression. To obtain the diagnostic value of these 2 circRNAs in HGG and LGG patients, a ROC curve analysis was conducted. The AUC was 0.8267 (95% CI: 0.6819–0.9714, p < 0.01) for hsa_circ_0000915 and 0.8044 (95% CI: 0.6457–0.9632, p < 0.001) for hsa_circ_0127664. Moreover, the diagnostic value of hsa_circ_0008362 and hsa_circ_0001467 was also evaluated by ROC curve analysis in HGG and normal tissue. The AUCs for hsa_circ_0008362 and hsa_circ_0001467 were 0.9467 (95% CI: 0.8728–1.000, p < 0.0001) and 0.9644 (95% CI: 0.9088–1.000, p < 0.0001), respectively. The potential diagnostic value of these circRNAs in glioma patients is displayed in Figure 3E.

GO enrichment and Reactome pathway analysis

By conducting Gene Ontology (GO) enrichment analysis in the biological process (BP), cellular component (CC), and molecular function (MF) categories, the host genes (linear counterparts) of the differentially regulated circRNAs in high-low grade were investigated, based on which their potential roles were deduced. The 10 most enriched BP, CC and MF GO terms of dysregulated circRNAs from the high-low grade glioma group are shown in Figure 4A. The regulation of neuron projection development, GTPase binding, and postsynaptic density were the most enriched GO entries in the BP, MF, and CC categories, respectively. Then, we performed Reactome pathway analysis, and 20 ranking predominant pathways are displayed in Figure 4B. According to the Reactome analysis, the top three enriched and meaningful pathways were signaling by Rho GTPases (Reactome, R-HSA-194315; p= 0.000312945), signaling by receptor tyrosine kinases (Reactome, R-HSA-9006934; p= 0.001761105) and transcriptional regulation by *TP53* (Reactome, R-HSA-3700989; p= 0.001084954).

Additionally, GO enrichment and Reactome pathway analysis of the downstream target genes in high-low grade was conducted. Figure 5A presents the 10 most enriched BP, CC and MF GO terms for the target genes in high-low grade. PremiRNA processing, ion channel activity, and RISC complex were the most enriched GO entries in the BP, MF, and CC categories, respectively. In addition, the top 20 predominant pathways were
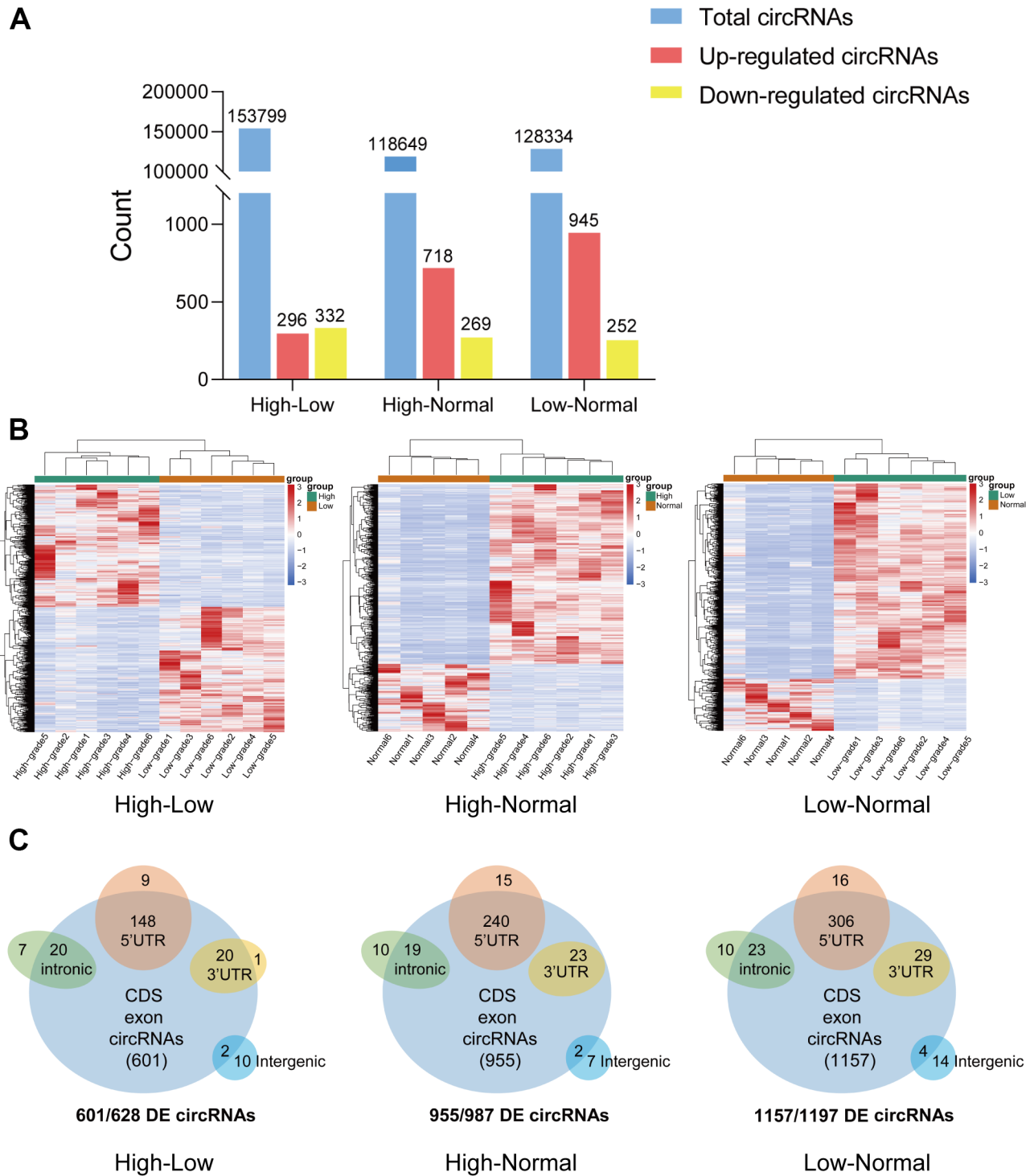

Figure 1. Overview of circRNA-seq profiles. (**A**) The quantity of total circRNAs and circRNAs with differential expression (upregulated and downregulated). (**B**) Hierarchical clustering heat map of differentially expressed circRNAs in the three groups. (**C**) CircRNAs with significant differential expression were classified by different genomic loci (exonic, intronic, antisense, intragenic, and intergenic).
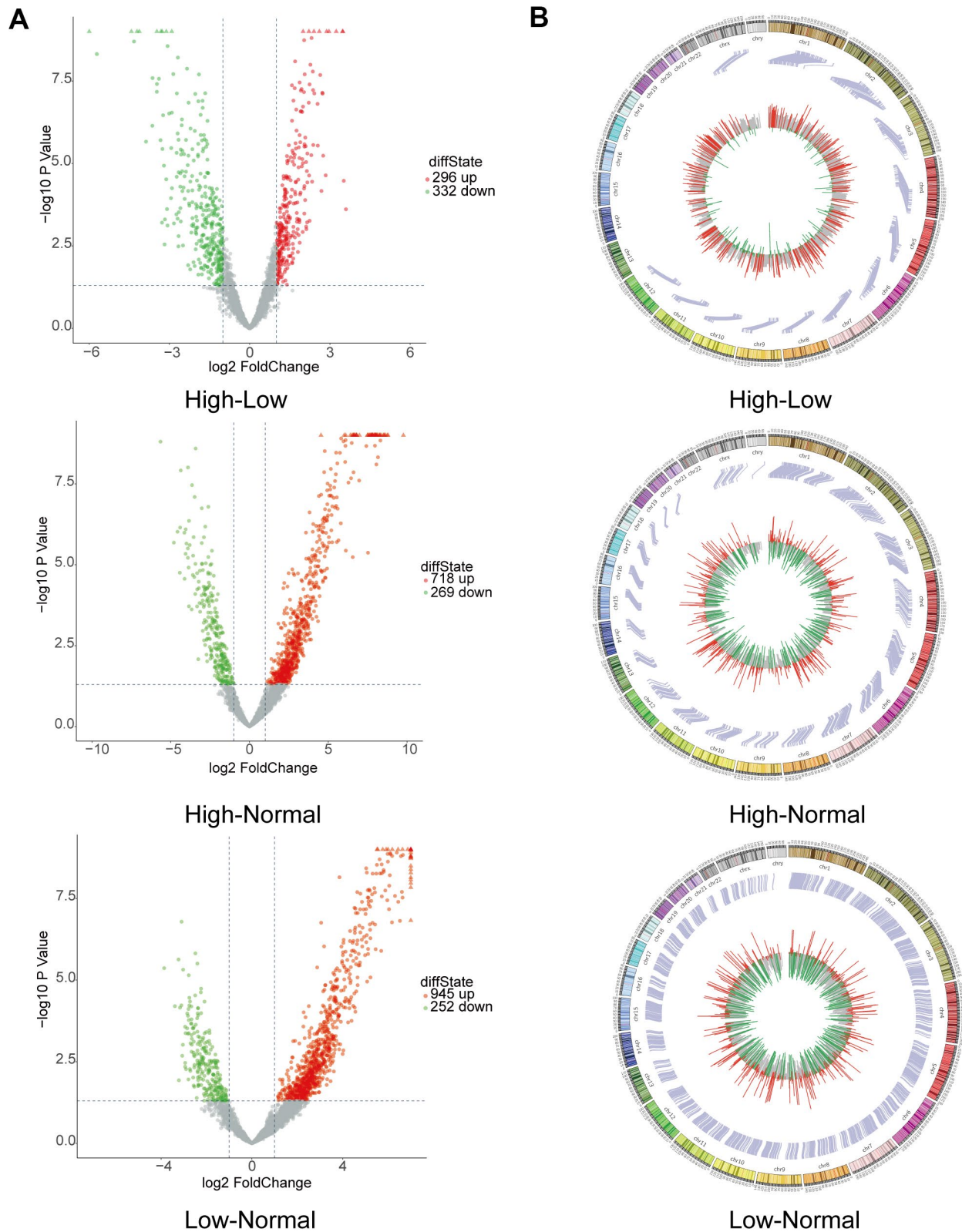
Figure 2. Bioinformatics analysis by RNA sequencing of circRNAs with differential expression. (**A**) Volcano plot depicting circRNAs. The volcano plot presents the expression profiles of each of the two groups. The vertical lines indicate a 2-fold (log2 scaled) increase and decrease in expression. The horizontal line indicates a p-value of 0.05 (−log10 scaled). CircRNAs showing significant upregulation are represented by red points. CircRNAs exhibiting significant downregulation are indicated by green points in the plot. (**B**) Circos plot revealing where each circRNA is located on human chromosomes.
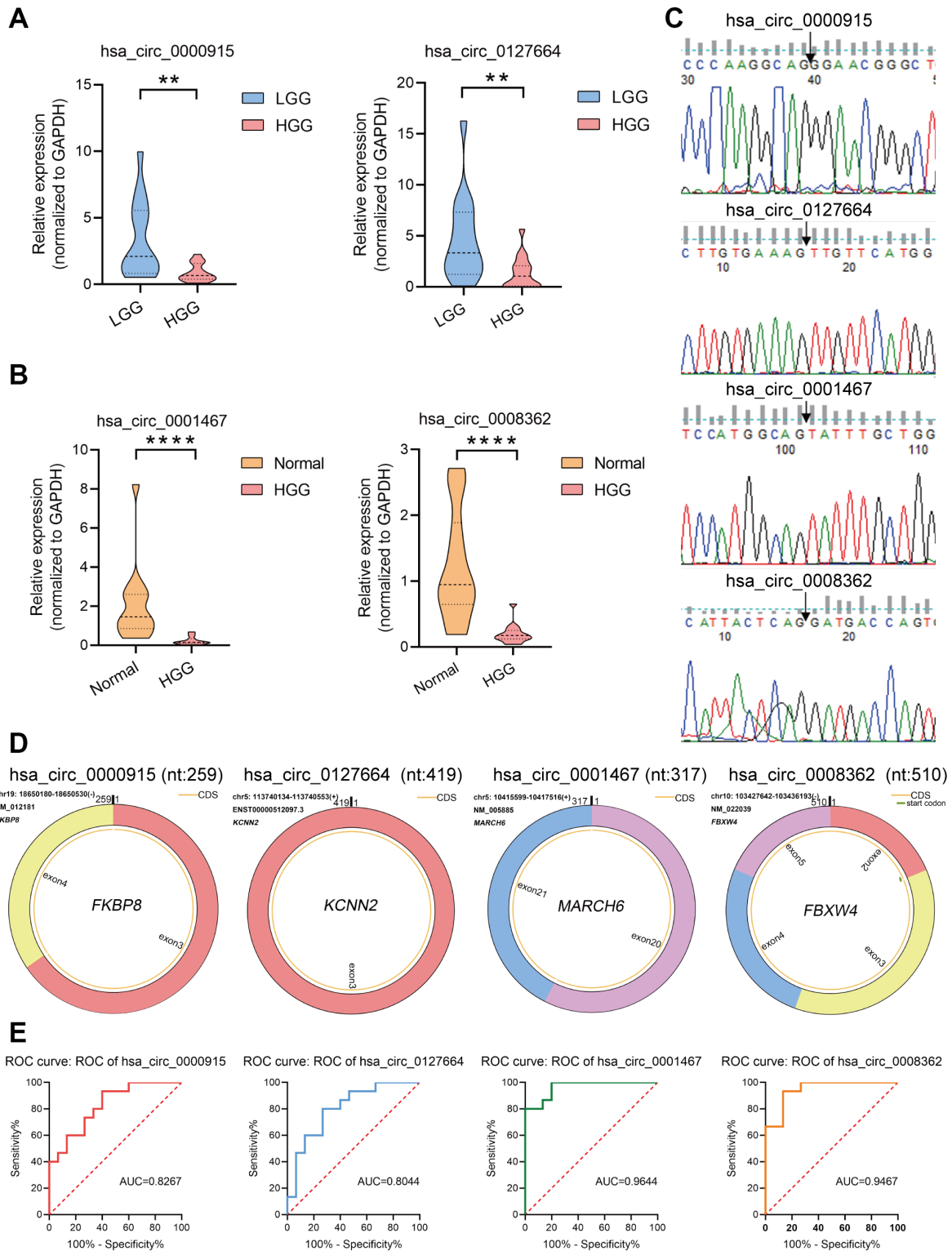
Figure 3. Verification of circRNA expression using qRT-PCR. (**A, B**) To confirm the downregulation of four circRNAs observed in circRNA-seq data, hsa_circ_0000915 and hsa_circ_0127664 were found to be downregulated in samples collected from 15 HGG and 15 LGG tissues, and hsa_circ_0001467 and hsa_circ_0008362 were found to be downregulated in 15 HGG tissues and 15 adjacent normal tissues via qRT-PCR. The data are presented as the means ± S.D. of a minimum of 3 independent experiments. *p < 0.05; **p < 0.01; ****p < 0.0001. (**C**) Head-to-tail splice junctions of 4 circRNAs confirmed by Sanger sequencing. (**D**) Characterization information for 4 candidate circRNAs. (**E**) ROC curve analysis of four candidate circRNAs. hsa_circ_0000915 and hsa_circ_0127664 in HGG patients were analyzed against low-grade glioma patients via ROC curves, and hsa_circ_0008362 and hsa_circ_0001467 in HGG were analyzed against normal tissue using ROC curves.
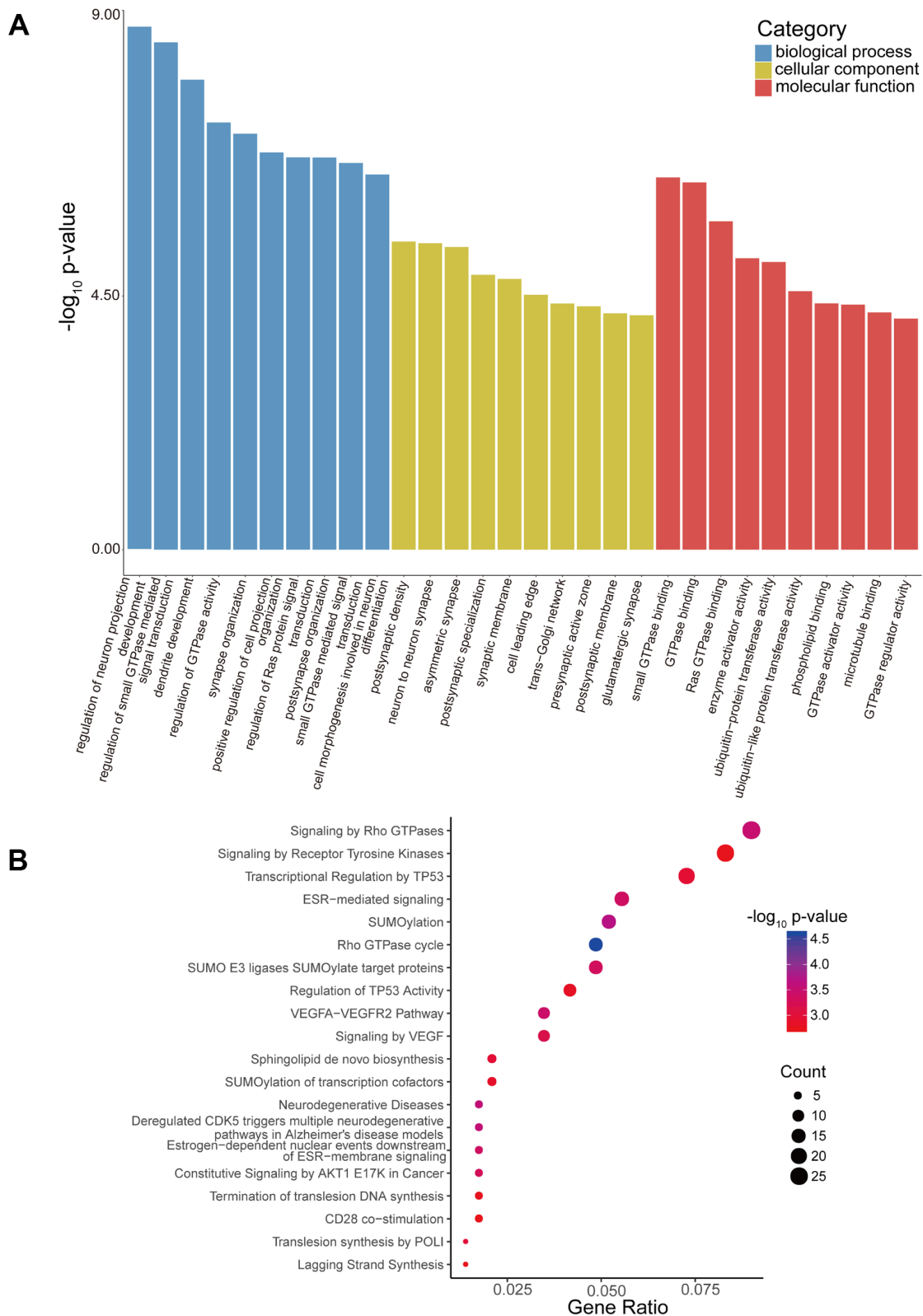
Figure 4. GO enrichment and Reactome pathway analyses of host genes of differentially expressed circRNAs. (**A**) GO enrichment analysis of host genes for circRNAs with differential expression. The ten most enriched GO terms in the MF, BP, and CC categories for the host genes. (**B**) Bubble map of Reactome pathway analysis of the top 20 predominant pathways. The X-axis denotes the enriched differential gene ratio in each pathway. The Y-axis represents the name of the significantly enriched pathway. The p-values are expressed by variations from red to blue. A deeper blue color indicates a greater significant difference.

displayed by Reactome pathway analysis (Figure 5B). According to the Reactome analysis, the top three pathways were cellular responses to stress (Reactome, R-HSA-2262752; p= 0.015340627), transcriptional regulation by *RUNX1* (Reactome, R-HSA-8878171; p=0.021079352) and transcriptional regulation by *MECP2* (Reactome, R-HSA-8986944; p=0.000234161).

CircRNA-miRNA-mRNA network analysis

Emerging studies have revealed that circRNAs could be miRNA sponges, which are effective in regulating how mRNA is expressed [23, 24]. In this paper, miRNAs that could potentially bind circRNAs were predicted using miRanda software (total score ≥ 150, total energy ≤ −20). A total of 129 miRNAs were found to be potential targets of the 4 identified circRNAs (Supplementary Table 2). Based on the bioinformatics analysis and combined with the research reports about miRNAs related to glioma in PubMed, we found that the most likely potential target miRNAs for hsa_circ_0000915 included hsa-miR-6765-3p and hsa-miR-330-5p. The most likely potential target miRNAs for hsa_circ_0127664 included hsa-miR-3945 and hsa-miR-99b-3p. hsa-miR-4656 and hsa-miR-217-5p were also predicted to be potential targets of hsa_circ_0008362. hsa-miR-6827-5p and hsa-miR-302d-5p were predicted to be potential targets of hsa_circ_0001467. The partially screened detailed sequence analysis of MREs for hsa_circ_0000915, hsa_circ_0127664, hsa_circ_0008362 and hsa_circ_0001467 is presented in Figure 6A.

In addition, 4 target miRNAs of 4 identified circRNAs were systematically analyzed using microRNA microarray data provided by the CGGA database (LGG group n = 60; HGG group n = 138), as they were extensively reported as mRNA regulators in gliomas. For the study, hsa-miR-330-5p, hsa-miR-99b-3p, hsa-miR-217-5p, and hsa-miR-302d-5p were taken as target miRNAs of these 4 circRNAs that had been discovered. hsa-miR-330-5p, hsa-miR-99b-3p, and hsa-miR-217-5p expression levels were found to show an increasing trend in the HGG group in comparison to the LGG group, but hsa-miR-302d-5p showed a decreasing trend. As shown by survival analysis, the group with enhanced hsa-miR-330-5p, hsa-miR-99b-3p, and hsa-miR-217-5p expression showed a reduced length of survival, and hsa-miR-302d-5p showed the opposite trend (Figure 6B).

The top target genes of miRNAs were predicted by TargetScan and miRDB (Criteria: Cumulative weighted context++ score ≤ −0.24 for TargetScan, Target Score ≥ 90 for miRDB). By analysis, we found that *FAIM2*, *DLGAP2*, *ATP1B1,* and *RALYL* could be the targets of hsa-miR-330-5p, hsa-miR-99b-3p, hsa-miR-217-5p and hsa-miR-302d-5p, respectively. We compared the expression levels of *FAIM2*, *DLGAP2*, *ATP1B1* and *RALYL* using ONCOMINE databases and found that these 4 genes were significantly downregulated in brain and CNS cancer compared with the normal group (Figure 7A). The expression data for these target genes in patients with GBM and LGG were examined by GEPIA. Compared with the normal group, *FAIM2*, *DLGAP2*, *ATP1B1* and *RALYL* were downregulated in GBM and LGG patients (Figure 7B, 7C).

The survival analysis was performed with the CGGA database. The group with low *FAIM2*, *DLGAP2*, *ATP1B1* and *RALYL* expression showed a reduced length of survival (Supplementary Figure 1A). We analyzed the *FAIM2*, *DLGAP2*, *ATP1B1* and *RALYL* alterations using the cBioPortal online tool for Glioblastoma Multiforme (TCGA, Firehose Legacy). Four genes were altered in 28 (21%) queried patients/samples (136 samples) (Supplementary Figure 1B). These results indicated that these genes were likely to be glioma-related tumor suppressor genes. The circRNA-miRNA-mRNA network was diagrammed with the assistance of Cytoscape software (Supplementary Figure 2) (Supplementary Table 3).

RBP binding and m⁶A modification function prediction

According to the data from the Cancer-Specific CircRNA Database (CSCD), RBPs binding with 4 identified circRNAs were drawn via Cytoscape software (Figure 8A). Twenty-two vital RBPs, IGF2BP1, IGF2BP3, EIF4A3, hnRNPC, and AGO2, can bind to circRNAs and may play important biological functions in glioma. According to the data from CSCD, the structure of 4 circRNAs was determined. Diagrams containing information about RBPs and ORFs are presented in Figure 8B. In addition, an interaction map of the difference in gene expression of RBPs between GBM and LGG and cancer pathway activity (activation and inhibition) was analyzed by GSCALite (Supplementary Figure 3). For example, we found that IGF2BP2, which is closely related to GBM and LGG, can be closely related to the mesenchymal transition (EMT) pathway of cancer progression.

According to data from the circBank database, the m⁶A levels for the 4 circRNAs were obtained and are shown in Table 1. We then analyzed their m⁶A modification sites using the SRAMP predictor tool. Only high confidence m⁶A sites are listed (Table 2). It was found that hsa_circ_0127664 and hsa_circ_0008362 had a relatively high m⁶A modification. The local m⁶A site structure visualization is displayed in Supplementary
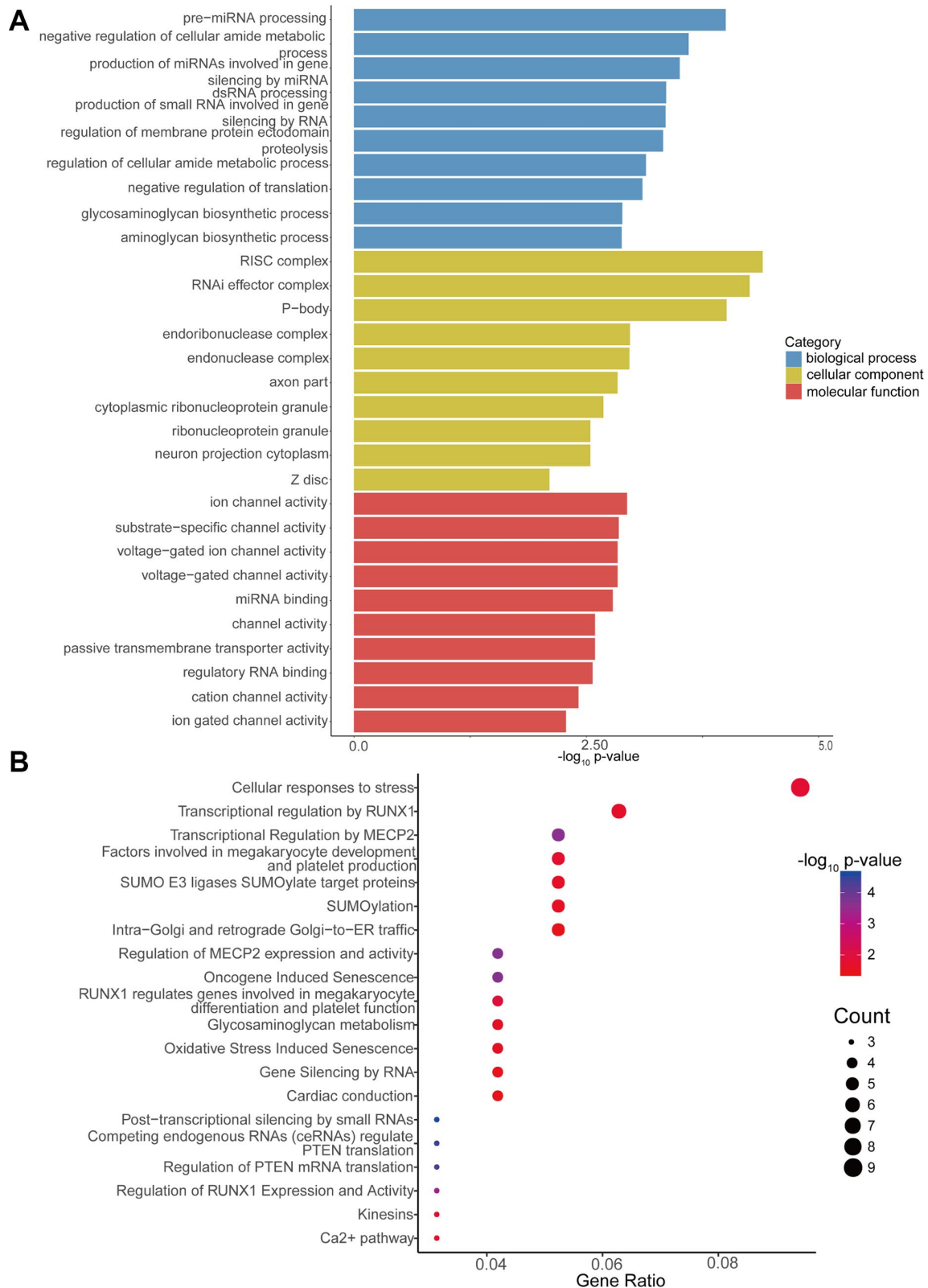
Figure 5. GO enrichment and Reactome pathway analyses of target genes of differentially expressed circRNAs. (**A**) GO enrichment analysis of target genes for circRNAs with differential expression. The 10 most significantly enriched GO terms in the MF, BP, and CC for the target genes of all miRNAs with differential expression. (**B**) Bubble map of Reactome pathway analysis of the top 20 predominant pathways. The X-axis denotes the enriched differential gene ratio in each pathway. The Y-axis represents the name of the significantly enriched pathway. The p-values are expressed as variations from red to blue. A deeper blue color indicates a greater significant difference.
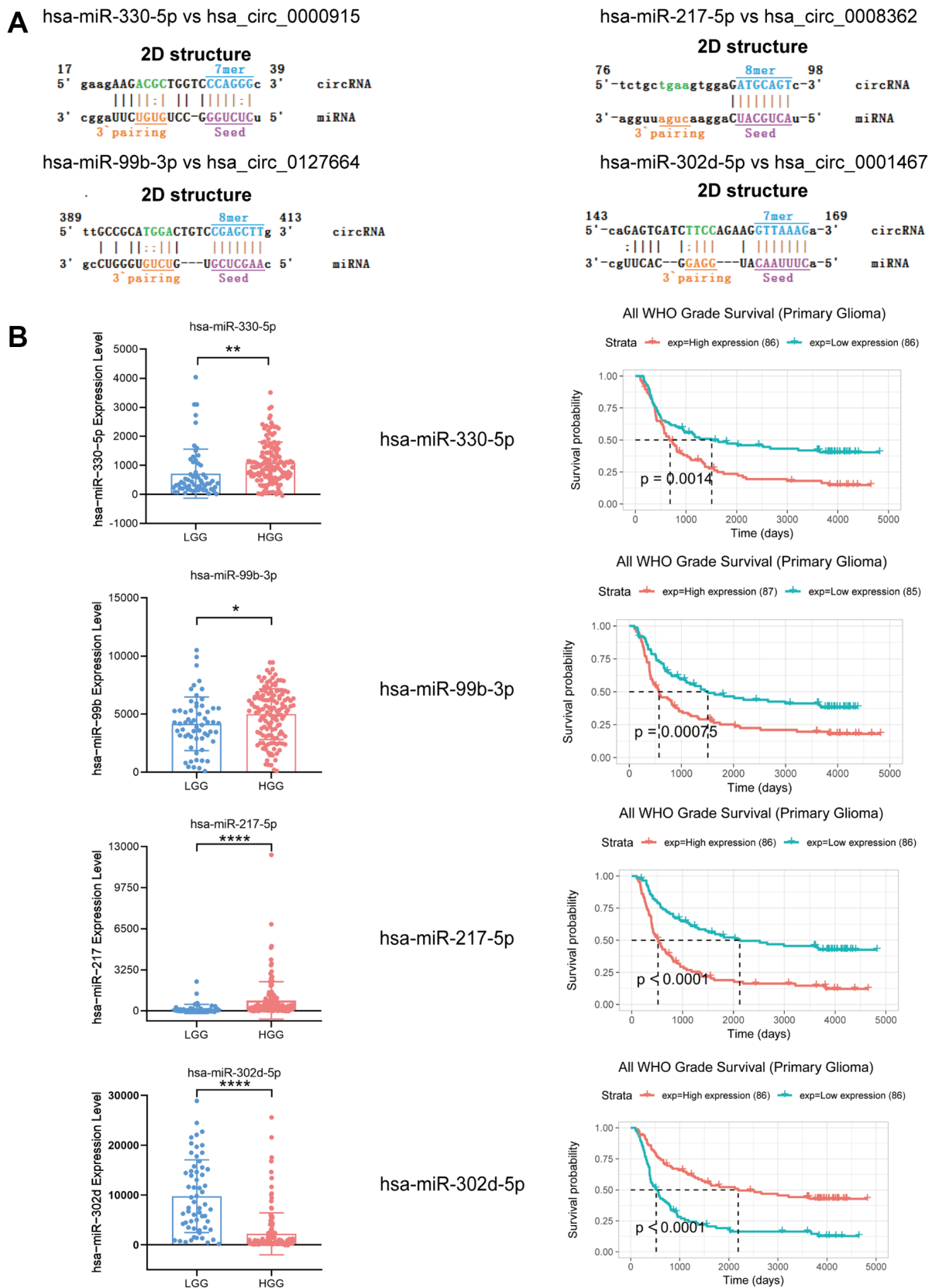
Figure 6. Expression and survival analysis of 4 target miRNAs and sequence analysis. (**A**) Sequence analysis results for MREs of identified circRNAs and target miRNAs. (**B**) In comparison to LGG patients, hsa-miR-330-5p, hsa-miR-99b-3p and hsa-miR-217-5p were upregulated in HGG, but hsa-miR-302d-5p was downregulated. Survival analysis of 4 target miRNAs. *p < 0.05; **p < 0.01; ****p < 0.0001.

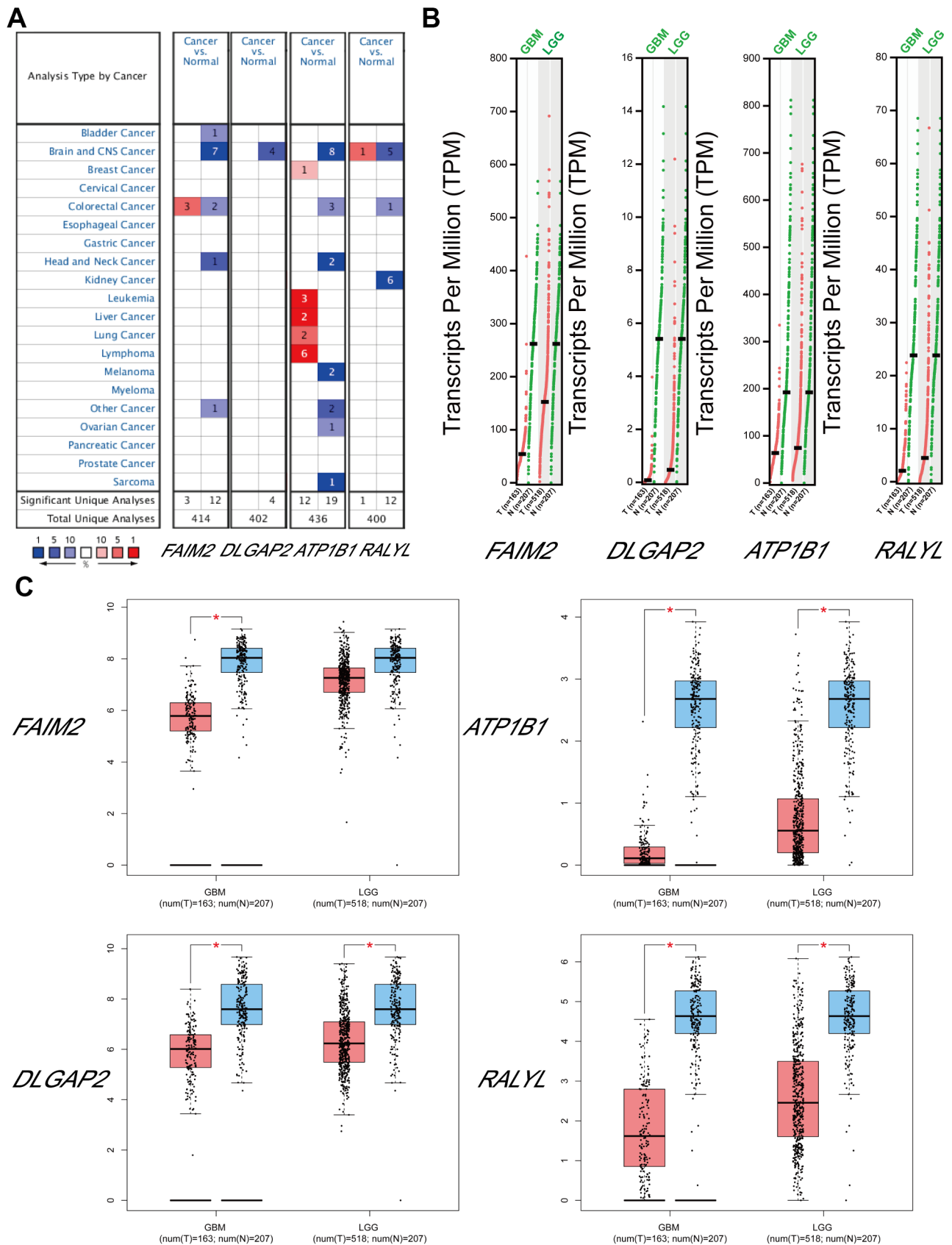**Figure 7. The expression levels of target mRNAs.** (**A**) The expression levels of *FAIM2*, *DLGAP2*, *ATP1B1* and *RALYL* in multiple cancers using ONCOMINE databases. (**B, C**) The expression levels of *FAIM2*, *DLGAP2*, *ATP1B1* and *RALYL* in GBM and LGG using GEPIA databases.

Figure 4. The prediction of coding proteins of identified circRNAs was analyzed by circRNADb, and hsa_circ_0000915 and hsa_circ_0001467 had IRES as well as ORFs, revealing their potential functions in coding proteins (Table 3).

DISCUSSION

Circular RNAs (circRNAs) have a critical regulatory function in human glioma [25]. As a detection method,

next-generation sequencing is a crucial method to explore novel circRNAs. However, regarding circRNA-seq data for glioma, most previous studies have focused on HGG, particularly glioblastoma (GBM, WHO IV), and thus, dysregulated circRNAs have only been analyzed between glioma and normal tissues [9]. The differentially expressed circRNAs of different grades of human glioma have not been fully investigated. Novel circRNAs related to different pathological grades of glioma and their crucial function are also worth
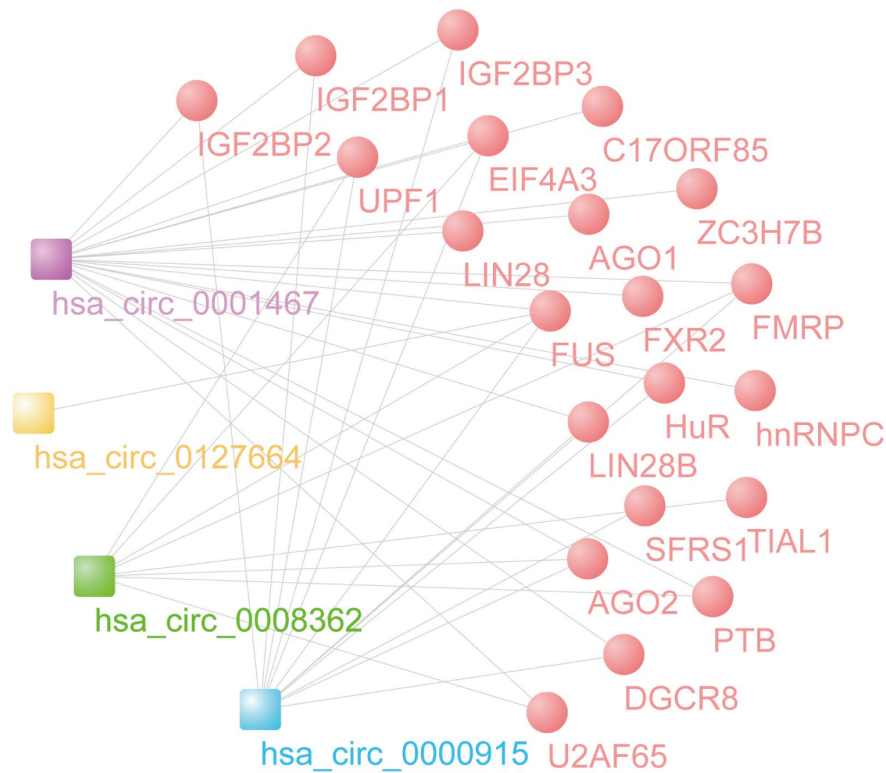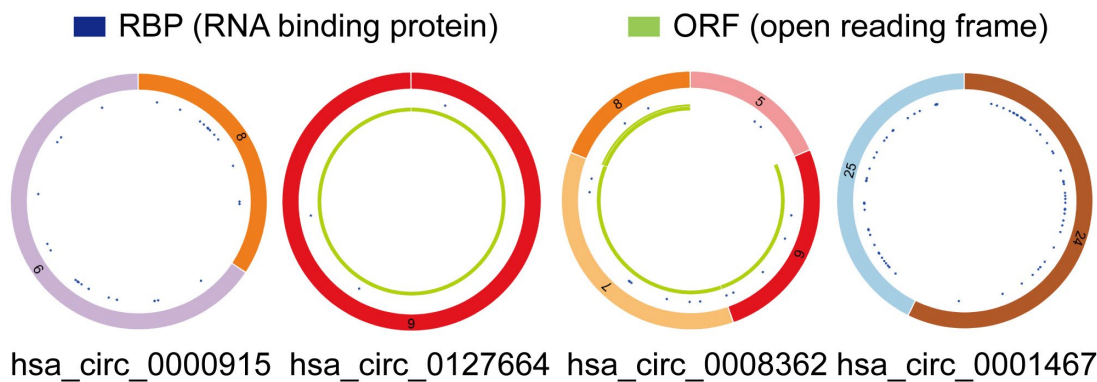

Figure 8. Prediction of RBP binding and m⁶A modification functions of selected circRNAs. (**A**) RBP binding to 4 identified circRNAs was predicted by CSCD data. (**B**) The structural patterns of 4 circRNAs analyzed using the CSCD database. All four circRNAs were searchable in the CSCD database. The RBP, and ORF information is shown.

Table 1. The m6A levels of circRNAs based on circBank.

circBase ID	circBank ID	chr	start	end	strand	m6A Levels
hsa_circ_0127664	hsa_circKCNN2_003	chr5	113740134	113740553	+	0.6784
hsa_circ_0008362	hsa_circFBXW4_008	chr10	103427642	103436193	-	0.0507
	hsa_circFBXW4_008	chr10	103432671	103436193	-	0.391
hsa_circ_0000915	hsa_circFKBP8_005	chr19	18650180	18650530	-	0.0521
	hsa_circFKBP8_005	chr19	18650180	18650530	-	0.0005
hsa_circ_0001467	hsa_circMARCH6_047	chr5	10415599	10417516	+	0.0005

Table 2. The m6A sites of circRNAs based on SRAMP.

circBase ID	Position	Sequence context	Score (combined)	Decision
hsa_circ_0127664	14	---------UUGUUCAUGGUGGACA AUGGAGCAGAUGACUGGAGA	0.626	m6A site (High confidence)
	400	AUUAUGGAUAAUUGCCGCAUG GACUGUCCGAGCUUGUGAAAG---	0.676	m6A site (High confidence)
hsa_circ_0008362	357	UCGGCUCAUGAACAGGAGGUGA ACUGUGUGGAUUGCAAAGGGGGC	0.637	m6A site (High confidence)
	402	AUCAUUGUGAGUGGCUCCAGGG ACAGGACGGCCAAGGUGUGGCCU	0.632	m6A site (High confidence)
	467	GCAGUGCUUACACACCAUCCAGA CUGAAGACCGAGUCUGGUCCAU	0.614	m6A site (High confidence)

Table 3. The coding potential prediction of the identified circRNAs.

circRNA ID	Gene symbol	Genomic length	Spliced length	Best transcript	Start position	End position	Protein length
hsa_circ_0000915	FKBP8	350	259	NM_012181	106	2r+154	188 aa
hsa_circ_0001467	MARCH6	1917	317	NM_005885	311	2r+21	114 aa

screening and prediction. In this research, we simultaneously investigated the circRNA expression profile of different grades of human glioma. Subsequently, to verify the RNA-seq data, the circRNA expression level in tissues was evaluated by qRT-PCR. To determine the potential clinical diagnostic value of circRNAs with differential expression, ROC curves were analyzed. In addition, to preliminarily explore the multilevel functions as well as potential mechanisms associated with malignant development of glioma, GO enrichment, Reactome pathway, and circRNA-miRNA-mRNA network analyses were performed. The expression and overall survival data for the target miRNAs and mRNAs were analyzed and examined using the GEPIA, CGGA, ONCOMINE, and cBioPortal databases. We screened 4 important circRNAs and predicted their potential functions. As a novel direction worth exploring for circRNAs, m6A modification levels,

RBPs, and ORFs were also predicted for further analysis.

We found that hundreds of circRNAs, with upregulation and downregulation, were significantly differentially expressed (FC ≥ 2 or ≤ 0.5 and $p < 0.05$) in different grade glioma patients. As revealed by the RNA-seq analysis carried out in the high-normal and low-normal groups, the number of upregulated circRNAs exceeded that of circRNAs exhibiting downregulation. The same phenomenon was observed in a study published by Xia et al. [26]. However, in the high-low group, we found more downregulated circRNAs, which aroused our interest. In addition, a large proportion of the circRNAs identified in our study originated from exons. In comparison, other circRNAs stemmed from intronic and/or intergenic genomic regions, which was also observed in a study published by Zhu et al. [27].

Despite many studies focusing on upregulated circRNAs in multiple cancer types, other studies have suggested that a majority of circRNAs with active expression play a significant role in normal physiological functions [28]. Relative to colorectal and ovarian cancer tissues, a high proportion of circRNAs are abundant in normal human tissues [29]. Many studies have revealed that certain circRNAs are downregulated in tumors compared with normal tissues and cells [30–33], which indicates that these circRNAs may function as suppressor genes and have a protective function in inhibiting cancer. Hence, we chose specific downregulated circRNAs for further research. Five downregulated circRNAs were first selected from the most downregulated circRNAs, and the RNA-seq reliability was evaluated with qRT-PCR. In 15 paired HGG and LGG tissues and 15 adjacent normal tissues, the expression of these 5 circRNAs was validated via RT-qPCR. Among the 5 circRNAs, four exhibited a clear conformance with RNA-seq, indicating that the RNA-seq data were reliable. Furthermore, we found that the selected representative circRNA, hsa_circ_0001467, was distinctly downregulated in glioma tissues, which is related to its diagnostic value for glioma patients and shows its potentially important clinical significance. Thus, downregulated circRNAs should not be neglected because they may serve as a novel tumor suppressive factor and potential target for new therapies in human cancer as well as other diseases [34–36].

The differential expression of circRNAs is reasonably related to their parental genes because they are mainly encoded from exons and/or introns of host genes [3, 37]. To explore the roles of circRNAs through this potential mechanism, the biological functions and identified predominant pathways of their host gene as well as target genes were conducted through GO enrichment and Reactome pathway analyses. According to GO enrichment analysis, the deregulation of circRNAs was related to the regulation of neuron projection development, GTPase binding, and postsynaptic density. According to the Reactome analysis of host genes, the top three pathways were signaling by Rho GTPases, signaling by receptor tyrosine kinases and transcriptional regulation by TP53. However, the top three pathways were cellular responses to stress, transcriptional regulation by RUNX1, and transcriptional regulation by MECP2 in the Reactome pathway analyses of target genes. We noted that the Rho GTPase pathway has been shown to be associated with infiltrative growth and invasion of glioblastoma [38, 39]. In addition, RUNX1 is considered to a key factor participating in the malignant biological behavior of glioma cells [40]. It is highly expressed and could contributes to the mesenchymal subtype of GBM in a TGFβ pathway-

dependent manner [41]. Although many studies have analyzed the host genes of dysregulated circRNAs based on GO enrichment and pathway analyses [27, 42], we support that GO and pathway analyses aimed at target genes can also better predict circRNA function.

Increasing evidence suggests that circRNAs are related to various diseases that humans can develop, particularly carcinomas, such as glioma [10], gastric cancer [43, 44], hepatocellular carcinoma [45–47], pancreatic cancer [48], thyroid carcinoma [49] and breast cancer [50]. Thus, it is speculated that circRNAs might assist with the diagnosis and treatment of these human diseases. Our results also revealed that these circRNAs were suitable and sensitive diagnostic markers in identifying glioma. Additionally, many studies have indicated that circRNA is capable of acting as a miRNA sponge, which leads to interference with miRNAs or other varieties of molecules associated with the target genes to be inhibited [23]. Considering the significance of miRNAs in the pathogenesis of glioma, it was suspected that the identified circRNAs might cause malignant development of glioma through interactions with miRNAs. Therefore, miRNAs targeted by these differentially expressed circRNAs were predicted. For instance, hsa_circ_0000915 has the potential to bind to hsa-miR-330-5p. As demonstrated in a prior study, hsa-miR-330-5p is related to the stemness and development of glioma [11]. In addition, according to our analysis based on the CGGA database, hsa-miR-330-5p also shows important clinical utility. A study on hsa-miR-302d-5p and glioblastoma showed that hsa-miR-302d-5p could function as a tumor inhibitor inhibiting glioblastoma via targeting NF-κB as well as *FGF2* [51]. In addition, miR-217 could target *YWHAG* and promote the viability, proliferation, migration, invasion and mitosis of glioblastoma cells both in vitro and in vivo [52]. Accordingly, the prediction results of circRNAs and miRNAs in this paper deserve further study.

By analysis, we found that *FAIM2*, *DLGAP2*, *ATP1B1* and *RALYL* could be the targets of hsa-miR-330-5p, hsa-miR-99b-3p, hsa-miR-217-5p and hsa-miR-302d-5p, respectively. The data from the GEPIA, CGGA, ONCOMINE, and cBioPortal databases all suggested that these four genes were closely related to glioma and are likely to be tumor suppressor genes.

RBPs can act as activators or inhibitors of circRNA formation and regulate the expression level of circRNAs [53]. Recently, binding to RBPs and the potential coding of circRNAs have attracted the attention of researchers; for example, circ-Amotl1 could bind to PDK1 as well as AKT1, facilitating the cardioprotective nuclear translocation of pAKT [54]. In

our research, the potential RBPs of these 4 circRNAs were analyzed. Twenty-two vital RBPs were found, including IGF2BP1, IGF2BP3, EIF4A3, hnRNPC, and AGO2. For instance, it was recently found that E2F1 and EIF4A3 might promote the biogenesis of circSEPT9 and the occurrence and development of triple-negative breast cancer by acting on the miR-637/LIF axis [55]. The interaction of the difference in gene expression of RBPs between GBM and LGG and cancer pathway activity was also analyzed. We found that some RBP genes were closely related to GBM and LGG, and they were predicted to have a close correlation with multiple cancer pathways. In our research, IGF2BP2 was predicted to be closely related to the EMT pathway of cancer progression. A recent study also confirmed this conclusion. It has been reported that miR-138 may function as a tumor inhibitor by directly inhibiting IGF2BP2 and suppressing EMT during the progression of LGG [56]. Hence, RBPs of circRNAs in this paper merit further study.

A large proportion of circRNAs, which are derived from coding genes and have ORFs, show potential functions of coding proteins [20]. In one study, circRNAs showed many m^{6}A consensus motifs, and a m^{6}A site was enough to initiate circRNA translation in a cap-independent fashion involving the m^{6}A reader YTHDF3 and the translation initiation factors eIF4G2 and eIF3A. circRNA translation efficiency can be affected by the level of m^{6}A modification [18, 57]. Interestingly, after searching the literature and GEPIA databases, it was found that eIF4G2 and YTHDF3 were upregulated in glioma compared with normal brain tissues [58] (GEPIA2 screening condition: log2foldchange cutoff=1, p-value cutoff=0.01). In another study, m^{6}A modification was also discovered to be common in circRNAs [59]. Recently, m^{6}A was reported to mediate the biogenesis of coding circRNAs [20] and could modulate cytoplasmic export and promote CRC liver metastasis [60]. The functional crosstalk and their function in tumor regulation between non-coding RNAs (miRNA, lncRNA, and circRNA) and m^{6}A have been explored [16, 61]. Hence, the analysis and validation of m^{6}A in circRNAs requires further research. We analyzed the m^{6}A modification levels of candidate circRNAs. For example, the m^{6}A modification level of hsa_circ_0127664 is 0.6784, which was provided by circBank. The coding proteins prediction of hsa_circ_0001467 suggests that it might function as a coding protein. Thus, this modification in circRNAs also merits further analysis.

CONCLUSIONS

Through next-generation sequencing and bioinformatics analysis, the important dysregulated circRNAs were

determined. Our findings indicated that 4 circRNAs (hsa_circ_0000915, hsa_circ_0127664, hsa_circ_0008362, and hsa_circ_0001467) are associated with the pathological characteristics of glioma and revealed critical regulatory functions at multiple levels. The results presented here might provide vital molecular biomarkers and potential therapeutic targets for glioma.

MATERIALS AND METHODS

Clinical samples

HGG and LGG patient tissues and adjacent normal tissues were collected from the Second Affiliated Hospital of Hebei Medical University and Affiliated Hospital of Hebei University. None of the recruited patients received preoperative radiotherapy or chemotherapy before biopsy. After resection from glioma patients, the tissues were instantly immersed in liquid nitrogen and then stored at -80°C for later use. The Ethics Committee of the Second Affiliated Hospital of Hebei Medical University and Affiliated Hospital of Hebei University authorized this study. Written informed consent was obtained under a grant from every glioma patient. Histopathological examination was independently confirmed by two pathologists.

Total RNA isolation and quality control

In line with the instructions from the manufacturer, a HiPure Total RNA Mini Kit (Magen) was employed to extract total RNA from tissues. In addition, a Eukaryote Total RNA Nano 6000 assay was used to assess RNA quality and integrity on an Agilent Technologies 2100 Bioanalyzer (Agilent, Santa Clara, CA, USA). RNA integrity numbers (RINs) were considered integrity values for RNA measurements. The results that showed RINs≥7 were kept for further analysis. After isolation, RNA was stored at -80°C for subsequent experiments.

RNA-seq analysis

To remove rRNA, the total RNA samples were treated with a RiboErase kit (Human/Mouse/Rat) (Kapa Biosystems, Inc., Woburn, MA). Before the RNA-seq libraries were constructed, linear RNAs were eliminated for subsequent treatment using RNase R (Epicenter Technologies, Madison, WI, USA). Briefly, as specified by the manufacturer, an RNA Hyper Prep Kit (Kapa Biosystems, Inc., Woburn, MA) was employed to construct strand-specific RNA-seq libraries. Following fragmentation, the digested RNA samples were applied to synthesize first- and second-strand cDNAs with the assistance of random hexamer primers; dTTP was substituted by dUTP in the second-strand synthesis

reaction. Subsequent to cDNA synthesis, end repair was carried out for the double-stranded products, a single 'A' base was added, and the cDNA products were ligated to adaptors. With the aid of magnetic particles, cDNA fragments were obtained for subsequent treatment using uracil DNA glycosylase to achieve removal of the second-strand cDNA. The first-strand cDNA was purified and then PCR-amplified, while a 2100 Agilent Bioanalyzer (Agilent, Santa Clara, CA, USA) was applied for quality control of the libraries. RNA-seq was performed with an Illumina HiSeq X Ten (X10) platform (Illumina, San Diego, CA, USA) via standard protocols on a 150-bp paired-end run. The information of relevant patients participating in the RNA-seq is presented in Supplementary Table 4.

Quantitative real-time PCR (qRT-PCR)

In line with the manufacturer's instructions, TRIzol reagent (Life Technologies, CA, USA) was employed to separate total RNA from tissues. Electrophoresis on a denaturing agarose gel was employed to assess RNA integrity. In addition, cDNA was acquired with a High-Capacity cDNA Reverse Transcription kit (Geneseed® II First Strand cDNA Synthesis Kit, Guangzhou, China). For qRT-PCR on an ABI 7500 real-time PCR system (Applied Biosystems, Foster City, CA, USA), a SYBR Green kit (Geneseed® qPCR SYBR® Green Master Mix, Guangzhou, China) was employed. For collection of fluorescent signals, the PCR program was operated for 5 minutes at 95°C prior to 40 thermal cycles, each with 10 sec at 95°C and 32 sec at 60°C. Glyceraldehyde phosphate dehydrogenase (GAPDH) (Sangon Biotech, Shanghai, China) was the endogenous control used to normalize circRNA expression. After PCR, the primer specificity was assessed by melt curve analysis. Using the average of the GAPDH-normalized $2^{-\Delta\Delta Ct}$ values, the circRNA expression levels were comparatively quantified through calculation [62]. The circRNA sequences were obtained from circBase (http://www.circbase.org/) [63] using divergent primers spanning the back-splice junction sites rather than convergent primers. A 1% (w/v) agarose gel was applied to separate the amplified PCR products, which were subjected to confirmation by Sanger sequencing.

Bioinformatics analysis

The functions and related pathways of the host genes (linear counterparts) and the downstream target genes (mRNA) of dysregulated circRNAs were separately investigated via GO (http://www.geneontology.org/) and Reactome pathway analyses (https://reactome.org/). The miRNAs could potentially bind the differentially expressed circRNAs identified with profiling data were predicted using miRanda [64] software coupled with statistical analysis. Four identified circRNAs and their related top miRNAs were drawn using Cytoscape software (version 3.7.1; http://www.cytoscape.org/). The TargetScan (http://www.targetscan.org/) and miRDB database (http://mirdb.org/) were applied to identify the miRNA-mRNA regulatory interactions. Expression and survival curves for selected target miRNAs and mRNAs were analyzed with microRNA microarray data from the Chinese Glioma Genome Atlas (CGGA) database. The expression and relevant data for target genes in patients with GBM and LGG were also examined from the GEPIA (http://gepia.cancer-pku.cn/), ONCOMINE (https://www.oncomine.org/), and cBioPortal (http://www.cbioportal.org/) databases. The cut-off of the ONCOMINE threshold of the p-value and fold change were defined as 0.0001 and 2, respectively. RBPs and ORF data matching with circRNAs were predicted via data from CSCD (http://gb.whu.edu.cn/CSCD/) [65]. The interaction of RBP genes and cancer pathways was analyzed by GSCALite (http://bioinfo.life.hust.edu.cn/web/GSCALite/). The m^6A levels and m^6A sites in these circRNAs were predicted via circBank (http://www.circbank.cn/) and SRAMP (http://www.cuilab.cn/sramp). The prediction of coding protein function of identified circRNAs was analyzed and predicted by circRNADb (http://reprod.njmu.edu.cn/circrnadb) [66].

Statistical analysis

GraphPad Prism 8 (GraphPad Software, Inc., La Jolla, CA, USA) was used for statistical analysis. Comparisons of two variables in the RNA-seq data were performed using the Student's t-test. Fold change (FC) ≥ 2 or ≤ 0.5 and $p < 0.05$ were considered statistically significant in the circRNA-seq analysis. To adjust the p-value in RNA-seq analysis, the false discovery rate was determined by calculations. For each circRNA, the expression level is indicated as the fold change determined by applying the $2^{-\Delta\Delta Ct}$ method for qRT-PCR analysis. All data are denoted as the mean ± S.D. of a minimum of three separate experiments. The Mann-Whitney test was used for data comparison. p-values < 0.05 indicate statistical significance.

Data Availability Statement

The raw data supporting the conclusions of this article will be made available by the authors, without undue reservation.

Abbreviations

BP: biological process; CC: cellular component; ceRNA: competing endogenous RNA; CGGA: Chinese

Glioma Genome Atlas; circRNA: circular RNA; EMT: mesenchymal transition; FC: fold change; GBM: glioblastoma; GO: Gene Ontology; HGG: high-grade glioma; IRES: internal ribosome entry site; LGG: low-grade glioma; m^{6}A: N6-methyladenosine; MF: molecular function; miRNA: microRNA; MRE: miRNA response element; ncRNA: endogenous noncoding RNA; ORF: open reading frame; qRT-PCR: quantitative real-time reverse transcription PCR; RBP: RNA binding protein; RIN: RNA integrity numbers; RNA-seq: RNA-sequencing.

AUTHOR CONTRIBUTIONS

XC G, YH Z, and Q L were the major contributors to the writing and revision of the manuscript. W X, XM L collected and prepared the samples. XC G, YH Z, and Q L contributed to performing the experiments and data interpretation. L S and WT Y collected the related references and participated in discussions. SG S and H W made substantial contributions to the conception or design of the work. SG S and H W approved the final version of the manuscript. All authors read and approved the final manuscript.

ACKNOWLEDGMENTS

CONFLICTS OF INTEREST

The authors have no other relevant affiliations or financial involvement with any organization or entity with a financial interest in or financial conflict with the subject matter or materials discussed in the manuscript apart from those disclosed.

FUNDING

REFERENCES

1. Louis DN, Perry A, Reifenberger G, von Deimling A, Figarella-Branger D, Cavenee WK, Ohgaki H, Wiestler OD, Kleihues P, Ellison DW. The 2016 world health organization classification of tumors of the central nervous system: a summary. Acta Neuropathol. 2016; 131:803–20.
https://doi.org/10.1007/s00401-016-1545-1
PMID:27157931

2. Jiang Y, He J, Guo Y, Tao H, Pu F, Li Y. Identification of genes related to low-grade glioma progression and prognosis based on integrated transcriptome analysis. J Cell Biochem. 2020; 121:3099–111.
https://doi.org/10.1002/jcb.29577
PMID:31886582

3. Chen LL, Yang L. Regulation of circRNA biogenesis. RNA Biol. 2015; 12:381–88.
https://doi.org/10.1080/15476286.2015.1020271
PMID:25746834

4. Qu S, Yang X, Li X, Wang J, Gao Y, Shang R, Sun W, Dou K, Li H. Circular RNA: a new star of noncoding RNAs. Cancer Lett. 2015; 365:141–48.
https://doi.org/10.1016/j.canlet.2015.06.003
PMID:26052092

5. Liu J, Zhao K, Huang N, Zhang N. Circular RNAs and human glioma. Cancer Biol Med. 2019; 16:11–23.
https://doi.org/10.20892/j.issn.2095-3941.2018.0425
PMID:31119043

6. Geng X, Jia Y, Zhang Y, Shi L, Li Q, Zang A, Wang H. Circular RNA: biogenesis, degradation, functions and potential roles in mediating resistance to anticarcinogens. Epigenomics. 2020; 12:267–83.
https://doi.org/10.2217/epi-2019-0295
PMID:31808351

7. Ding C, Yi X, Wu X, Bu X, Wang D, Wu Z, Zhang G, Gu J, Kang D. Exosome-mediated transfer of circRNA CircNFIX enhances temozolomide resistance in glioma. Cancer Lett. 2020; 479:1–12.
https://doi.org/10.1016/j.canlet.2020.03.002
PMID:32194140

8. Zhang S, Liao K, Miao Z, Wang Q, Miao Y, Guo Z, Qiu Y, Chen B, Ren L, Wei Z, Lin Y, Lu X, Qiu Y. CircFOXO3 promotes glioblastoma progression by acting as a competing endogenous RNA for NFAT5. Neuro Oncol. 2019; 21:1284–96.
https://doi.org/10.1093/neuonc/noz128
PMID:31504797

9. Wang R, Zhang S, Chen X, Li N, Li J, Jia R, Pan Y, Liang H. CircNT5E acts as a sponge of miR-422a to promote glioblastoma tumorigenesis. Cancer Res. 2018; 78:4812–25.

https://doi.org/10.1158/0008-5472.CAN-18-0532
PMID:29967262

10. Lu Y, Deng X, Xiao G, Zheng X, Ma L, Huang W. Circ_0001730 promotes proliferation and invasion via the miR-326/Wnt7B axis in glioma cells. Epigenomics. 2019; 11:1335–52.
https://doi.org/10.2217/epi-2019-0121
PMID:31304776

11. Chen J, Chen T, Zhu Y, Li Y, Zhang Y, Wang Y, Li X, Xie X, Wang J, Huang M, Sun X, Ke Y. circPTN sponges miR-145-5p/miR-330-5p to promote proliferation and stemness in glioma. J Exp Clin Cancer Res. 2019; 38:398.
https://doi.org/10.1186/s13046-019-1376-8
PMID:31511040

12. Luo Z, Rong Z, Zhang J, Zhu Z, Yu Z, Li T, Fu Z, Qiu Z, Huang C. Circular RNA circCCDC9 acts as a miR-6792-3p sponge to suppress the progression of gastric cancer through regulating CAV1 expression. Mol Cancer. 2020; 19:86.
https://doi.org/10.1186/s12943-020-01203-8
PMID:32386516

13. He J, Huang Z, He M, Liao J, Zhang Q, Wang S, Xie L, Ouyang L, Koeffler HP, Yin D, Liu A. Circular RNA MAPK4 (circ-MAPK4) inhibits cell apoptosis via MAPK signaling pathway by sponging miR-125a-3p in gliomas. Mol Cancer. 2020; 19:17.
https://doi.org/10.1186/s12943-019-1120-1
PMID:31992303

14. Han B, Chao J, Yao H. Circular RNA and its mechanisms in disease: from the bench to the clinic. Pharmacol Ther. 2018; 187:31–44.
https://doi.org/10.1016/j.pharmthera.2018.01.010
PMID:29406246

15. Zhang M, Huang N, Yang X, Luo J, Yan S, Xiao F, Chen W, Gao X, Zhao K, Zhou H, Li Z, Ming L, Xie B, Zhang N. A novel protein encoded by the circular form of the SHPRH gene suppresses glioma tumorigenesis. Oncogene. 2018; 37:1805–14.
https://doi.org/10.1038/s41388-017-0019-9
PMID:29343848

16. Zhang Y, Geng X, Li Q, Xu J, Tan Y, Xiao M, Song J, Liu F, Fang C, Wang H. m6A modification in RNA: biogenesis, functions and roles in gliomas. J Exp Clin Cancer Res. 2020; 39:192.
https://doi.org/10.1186/s13046-020-01706-8
PMID:32943100

17. Li F, Yi Y, Miao Y, Long W, Long T, Chen S, Cheng W, Zou C, Zheng Y, Wu X, Ding J, Zhu K, Chen D, et al. N[6]-methyladenosine modulates nonsense-mediated mRNA decay in human glioblastoma. Cancer Res. 2019; 79:5785–98.

https://doi.org/10.1158/0008-5472.CAN-18-2868
PMID:31530567

18. Yang Y, Fan X, Mao M, Song X, Wu P, Zhang Y, Jin Y, Yang Y, Chen LL, Wang Y, Wong CC, Xiao X, Wang Z. Extensive translation of circular RNAs driven by N[6]-methyladenosine. Cell Res. 2017; 27:626–41.
https://doi.org/10.1038/cr.2017.31 PMID:28281539

19. Tang C, Klukovich R, Peng H, Wang Z, Yu T, Zhang Y, Zheng H, Klungland A, Yan W. ALKBH5-dependent m6A demethylation controls splicing and stability of long 3'-UTR mRNAs in male germ cells. Proc Natl Acad Sci USA. 2018; 115:E325–33.
https://doi.org/10.1073/pnas.1717794115
PMID:29279410

20. Tang C, Xie Y, Yu T, Liu N, Wang Z, Woolsey RJ, Tang Y, Zhang X, Qin W, Zhang Y, Song G, Zheng W, Wang J, et al. m[6]A-dependent biogenesis of circular RNAs in male germ cells. Cell Res. 2020; 30:211–28.
https://doi.org/10.1038/s41422-020-0279-8
PMID:32047269

21. Huang R, Zhang Y, Bai Y, Han B, Ju M, Chen B, Yang L, Wang Y, Zhang H, Zhang H, Xie C, Zhang Z, Yao H. N[6]-methyladenosine modification of fatty acid amide hydrolase messenger RNA in circular RNA STAG1-regulated astrocyte dysfunction and depressive-like behaviors. Biol Psychiatry. 2020; 88:392–404.
https://doi.org/10.1016/j.biopsych.2020.02.018
PMID:32387133

22. Zhong S, Wang J, Zhang Q, Xu H, Feng J. CircPrimer: a software for annotating circRNAs and determining the specificity of circRNA primers. BMC Bioinformatics. 2018; 19:292.
https://doi.org/10.1186/s12859-018-2304-1
PMID:30075703

23. Hansen TB, Jensen TI, Clausen BH, Bramsen JB, Finsen B, Damgaard CK, Kjems J. Natural RNA circles function as efficient microRNA sponges. Nature. 2013; 495:384–88.
https://doi.org/10.1038/nature11993 PMID:23446346

24. Shan K, Liu C, Liu BH, Chen X, Dong R, Liu X, Zhang YY, Liu B, Zhang SJ, Wang JJ, Zhang SH, Wu JH, Zhao C, Yan B. Circular noncoding RNA HIPK3 mediates retinal vascular dysfunction in diabetes mellitus. Circulation. 2017; 136:1629–42.
https://doi.org/10.1161/CIRCULATIONAHA.117.029004 PMID:28860123

25. Zhang Y, Lin X, Geng X, Shi L, Li Q, Liu F, Fang C, Wang H. Advances in circular RNAs and their role in glioma (review). Int J Oncol. 2020; 57:67–79.
https://doi.org/10.3892/ijo.2020.5049 PMID:32319596

26. Xia X, Li X, Li F, Wu X, Zhang M, Zhou H, Huang N, Yang X, Xiao F, Liu D, Yang L, Zhang N. A novel tumor

suppressor protein encoded by circular AKT3 RNA inhibits glioblastoma tumorigenicity by competing with active phosphoinositide-dependent Kinase-1. Mol Cancer. 2019; 18:131.
https://doi.org/10.1186/s12943-019-1056-5

27. Kun-Peng Z, Xiao-Long M, Lei Z, Chun-Lin Z, Jian-Ping H, Tai-Cheng Z. Screening circular RNA related to chemotherapeutic resistance in osteosarcoma by RNA sequencing. Epigenomics. 2018; 10:1327–46.
https://doi.org/10.2217/epi-2018-0023
PMID:30191736

28. Song X, Zhang N, Han P, Moon BS, Lai RK, Wang K, Lu W. Circular RNA profile in gliomas revealed by identification tool UROBORUS. Nucleic Acids Res. 2016; 44:e87.
https://doi.org/10.1093/nar/gkw075 PMID:26873924

29. Bachmayr-Heyda A, Reiner AT, Auer K, Sukhbaatar N, Aust S, Bachleitner-Hofmann T, Mesteri I, Grunt TW, Zeillinger R, Pils D. Correlation of circular RNA abundance with proliferation—exemplified with colorectal and ovarian cancer, idiopathic lung fibrosis, and normal human tissues. Sci Rep. 2015; 5:8057.
https://doi.org/10.1038/srep08057 PMID:25624062

30. Zhang PF, Wei CY, Huang XY, Peng R, Yang X, Lu JC, Zhang C, Gao C, Cai JB, Gao PT, Gao DM, Shi GM, Ke AW, Fan J. Circular RNA circTRIM33-12 acts as the sponge of MicroRNA-191 to suppress hepatocellular carcinoma progression. Mol Cancer. 2019; 18:105.
https://doi.org/10.1186/s12943-019-1031-1
PMID:31153371

31. Liu H, Bi J, Dong W, Yang M, Shi J, Jiang N, Lin T, Huang J. Invasion-related circular RNA circFNDC3B inhibits bladder cancer progression through the miR-1178-3p/G3BP2/SRC/FAK axis. Mol Cancer. 2018; 17:161.
https://doi.org/10.1186/s12943-018-0908-8
PMID:30458784

32. Dong W, Bi J, Liu H, Yan D, He Q, Zhou Q, Wang Q, Xie R, Su Y, Yang M, Lin T, Huang J. Circular RNA ACVR2A suppresses bladder cancer cells proliferation and metastasis through miR-626/EYA4 axis. Mol Cancer. 2019; 18:95.
https://doi.org/10.1186/s12943-019-1025-z
PMID:31101108

33. Kong Y, Li Y, Luo Y, Zhu J, Zheng H, Gao B, Guo X, Li Z, Chen R, Chen C. circNFIB1 inhibits lymphangiogenesis and lymphatic metastasis via the miR-486-5p/PIK3R1/VEGF-C axis in pancreatic cancer. Mol Cancer. 2020; 19:82.
https://doi.org/10.1186/s12943-020-01205-6
PMID:32366257

34. Zhao Q, Liu J, Deng H, Ma R, Liao JY, Liang H, Hu J, Li J, Guo Z, Cai J, Xu X, Gao Z, Su S. Targeting mitochondria-located circRNA SCAR alleviates NASH via reducing mROS output. Cell. 2020; 183:76–93.e22.
https://doi.org/10.1016/j.cell.2020.08.009
PMID:32931733

35. Han D, Wang Y, Wang Y, Dai X, Zhou T, Chen J, Tao B, Zhang J, Cao F. The tumor-suppressive human circular RNA CircITCH sponges miR-330-5p to ameliorate doxorubicin-induced cardiotoxicity through upregulating SIRT6, survivin, and SERCA2a. Circ Res. 2020; 127:e108–25.
https://doi.org/10.1161/CIRCRESAHA.119.316061
PMID:32392088

36. Isik A, Ramanathan R. Approaches to the treatment of pilonidal sinus disease, clinical practice in 2019. Int Wound J. 2020; 17:508–09.
https://doi.org/10.1111/iwj.13265 PMID:31710171

37. Geng X, Lin X, Zhang Y, Li Q, Guo Y, Fang C, Wang H. Exosomal circular RNA sorting mechanisms and their function in promoting or inhibiting cancer. Oncol Lett. 2020; 19:3369–80.
https://doi.org/10.3892/ol.2020.11449
PMID:32269609

38. Wang H, Han M, Whetsell W Jr, Wang J, Rich J, Hallahan D, Han Z. Tax-interacting protein 1 coordinates the spatiotemporal activation of Rho GTPases and regulates the infiltrative growth of human glioblastoma. Oncogene. 2014; 33:1558–69.
https://doi.org/10.1038/onc.2013.97 PMID:23563176

39. Pettee KM, Becker KN, Alberts AS, Reinard KA, Schroeder JL, Eisenmann KM. Targeting the mDia formin-assembled cytoskeleton is an effective anti-invasion strategy in adult high-grade glioma patient-derived neurospheres. Cancers (Basel). 2019; 11:392.
https://doi.org/10.3390/cancers11030392
PMID:30897774

40. Teng H, Wang P, Xue Y, Liu X, Ma J, Cai H, Xi Z, Li Z, Liu Y. Role of HCP5-miR-139-RUNX1 feedback loop in regulating Malignant behavior of glioma cells. Mol Ther. 2016; 24:1806–22.
https://doi.org/10.1038/mt.2016.103 PMID:27434586

41. Zhao K, Cui X, Wang Q, Fang C, Tan Y, Wang Y, Yi K, Yang C, You H, Shang R, Wang J, Kang C. RUNX1 contributes to the mesenchymal subtype of glioblastoma in a TGFβ pathway-dependent manner. Cell Death Dis. 2019; 10:877.
https://doi.org/10.1038/s41419-019-2108-x
PMID:31754093

42. Xu C, Yu Y, Ding F. Microarray analysis of circular RNA expression profiles associated with gemcitabine resistance in pancreatic cancer cells. Oncol Rep. 2018; 40:395–404.
https://doi.org/10.3892/or.2018.6450 PMID:29781033

---

43. Zhang J, Liu H, Hou L, Wang G, Zhang R, Huang Y, Chen X, Zhu J. Circular RNA_LARP4 inhibits cell proliferation and invasion of gastric cancer by sponging miR-424-5p and regulating LATS1 expression. Mol Cancer. 2017; 16:151.
https://doi.org/10.1186/s12943-017-0719-3
PMID:28893265

44. Huang X, Li Z, Zhang Q, Wang W, Li B, Wang L, Xu Z, Zeng A, Zhang X, Zhang X, He Z, Li Q, Sun G, et al. Circular RNA AKT3 upregulates PIK3R1 to enhance cisplatin resistance in gastric cancer via miR-198 suppression. Mol Cancer. 2019; 18:71.
https://doi.org/10.1186/s12943-019-0969-3
PMID:30927924

45. Yu J, Xu QG, Wang ZG, Yang Y, Zhang L, Ma JZ, Sun SH, Yang F, Zhou WP. Circular RNA cSMARCA5 inhibits growth and metastasis in hepatocellular carcinoma. J Hepatol. 2018; 68:1214–27.
https://doi.org/10.1016/j.jhep.2018.01.012
PMID:29378234

46. Liang WC, Wong CW, Liang PP, Shi M, Cao Y, Rao ST, Tsui SK, Waye MM, Zhang Q, Fu WM, Zhang JF. Translation of the circular RNA circβ-catenin promotes liver cancer cell growth through activation of the Wnt pathway. Genome Biol. 2019; 20:84.
https://doi.org/10.1186/s13059-019-1685-4
PMID:31027518

47. Han D, Li J, Wang H, Su X, Hou J, Gu Y, Qian C, Lin Y, Liu X, Huang M, Li N, Zhou W, Yu Y, Cao X. Circular RNA circMTO1 acts as the sponge of microRNA-9 to suppress hepatocellular carcinoma progression. Hepatology. 2017; 66:1151–64.
https://doi.org/10.1002/hep.29270
PMID:28520103

48. Li Z, Yanfang W, Li J, Jiang P, Peng T, Chen K, Zhao X, Zhang Y, Zhen P, Zhu J, Li X. Tumor-released exosomal circular RNA PDE8A promotes invasive growth via the miR-338/MACC1/MET pathway in pancreatic cancer. Cancer Lett. 2018; 432:237–50.
https://doi.org/10.1016/j.canlet.2018.04.035
PMID:29709702

49. Liu F, Zhang J, Qin L, Yang Z, Xiong J, Zhang Y, Li R, Li S, Wang H, Yu B, Zhao W, Wang W, Li Z, Liu J. Circular RNA EIF6 (Hsa_circ_0060060) sponges miR-144-3p to promote the cisplatin-resistance of human thyroid carcinoma cells by autophagy regulation. Aging (Albany NY). 2018; 10:3806–20.
https://doi.org/10.18632/aging.101674
PMID:30540564

50. Wang J, Zhang Q, Zhou S, Xu H, Wang D, Feng J, Zhao J, Zhong S. Circular RNA expression in exosomes derived from breast cancer cells and patients. Epigenomics. 2019; 11:411–21.
https://doi.org/10.2217/epi-2018-0111
PMID:30785332

51. Wang F, Yang L, Sun J, Zheng J, Shi L, Zhang G, Cui N. Tumor suppressors microRNA-302d and microRNA-16 inhibit human glioblastoma multiforme by targeting NF-κB and FGF2. Mol Biosyst. 2017; 13:1345–54.
https://doi.org/10.1039/c7mb00139h PMID:28497156

52. Wang H, Zhi H, Ma D, Li T. MiR-217 promoted the proliferation and invasion of glioblastoma by repressing YWHAG. Cytokine. 2017; 92:93–102.
https://doi.org/10.1016/j.cyto.2016.12.013
PMID:28126486

53. Du WW, Zhang C, Yang W, Yong T, Awan FM, Yang BB. Identifying and characterizing circRNA-protein interaction. Theranostics. 2017; 7:4183–91.
https://doi.org/10.7150/thno.21299 PMID:29158818

54. Zeng Y, Du WW, Wu Y, Yang Z, Awan FM, Li X, Yang W, Zhang C, Yang Q, Yee A, Chen Y, Yang F, Sun H, et al. A circular RNA binds to and activates AKT phosphorylation and nuclear localization reducing apoptosis and enhancing cardiac repair. Theranostics. 2017; 7:3842–55.
https://doi.org/10.7150/thno.19764 PMID:29109781

55. Zheng X, Huang M, Xing L, Yang R, Wang X, Jiang R, Zhang L, Chen J. The circRNA circSEPT9 mediated by E2F1 and EIF4A3 facilitates the carcinogenesis and development of triple-negative breast cancer. Mol Cancer. 2020; 19:73.
https://doi.org/10.1186/s12943-020-01183-9
PMID:32264877

56. Yang Y, Liu X, Cheng L, Li L, Wei Z, Wang Z, Han G, Wan X, Wang Z, Zhang J, Chen C. Tumor suppressor microRNA-138 suppresses low-grade glioma development and metastasis via regulating IGF2BP2. Onco Targets Ther. 2020; 13:2247–60.
https://doi.org/10.2147/OTT.S232795 PMID:32214825

57. Di Timoteo G, Dattilo D, Centrón-Broco A, Colantoni A, Guarnacci M, Rossi F, Incarnato D, Oliviero S, Fatica A, Morlando M, Bozzoni I. Modulation of circRNA metabolism by m^{6}A modification. Cell Rep. 2020; 31:107641.
https://doi.org/10.1016/j.celrep.2020.107641
PMID:32402287

58. Chai Y, Xie M. LINC01579 promotes cell proliferation by acting as a ceRNA of miR-139-5p to upregulate EIF4G2 expression in glioblastoma. J Cell Physiol. 2019; 234:23658–66.
https://doi.org/10.1002/jcp.28933 PMID:31187495

59. Zhou C, Molinie B, Daneshvar K, Pondick JV, Wang J, Van Wittenberghe N, Xing Y, Giallourakis CC, Mullen AC. Genome-wide maps of m6A circRNAs identify widespread and cell-type-specific methylation patterns

that are distinct from mRNAs. Cell Rep. 2017; 20:2262–76.
https://doi.org/10.1016/j.celrep.2017.08.027
PMID:28854373

60. Chen RX, Chen X, Xia LP, Zhang JX, Pan ZZ, Ma XD, Han K, Chen JW, Judde JG, Deas O, Wang F, Ma NF, Guan X, et al. N[6]-methyladenosine modification of circNSUN2 facilitates cytoplasmic export and stabilizes HMGA2 to promote colorectal liver metastasis. Nat Commun. 2019; 10:4695.
https://doi.org/10.1038/s41467-019-12651-2
PMID:31619685

61. Dai F, Wu Y, Lu Y, An C, Zheng X, Dai L, Guo Y, Zhang L, Li H, Xu W, Gao W. Crosstalk between RNA m[6]A modification and non-coding RNA contributes to cancer growth and progression. Mol Ther Nucleic Acids. 2020; 22:62–71.
https://doi.org/10.1016/j.omtn.2020.08.004
PMID:32911345

62. Livak KJ, Schmittgen TD. Analysis of relative gene expression data using real-time quantitative PCR and the 2(-Delta Delta C(T)) method. Methods. 2001; 25:402–08.
https://doi.org/10.1006/meth.2001.1262
PMID:11846609

63. Glažar P, Papavasileiou P, Rajewsky N. circBase: a database for circular RNAs. RNA. 2014; 20:1666–70.
https://doi.org/10.1261/rna.043687.113
PMID:25234927

64. Betel D, Wilson M, Gabow A, Marks DS, Sander C. The microRNA.org resource: targets and expression. Nucleic Acids Res. 2008; 36:D149–53.
https://doi.org/10.1093/nar/gkm995 PMID:18158296

65. Xia S, Feng J, Chen K, Ma Y, Gong J, Cai F, Jin Y, Gao Y, Xia L, Chang H, Wei L, Han L, He C. CSCD: a database for cancer-specific circular RNAs. Nucleic Acids Res. 2018; 46:D925–29.
https://doi.org/10.1093/nar/gkx863
PMID:29036403

66. Chen X, Han P, Zhou T, Guo X, Song X, Li Y. circRNADb: a comprehensive database for human circular RNAs with protein-coding annotations. Sci Rep. 2016; 6:34985.
https://doi.org/10.1038/srep34985
PMID:27725737
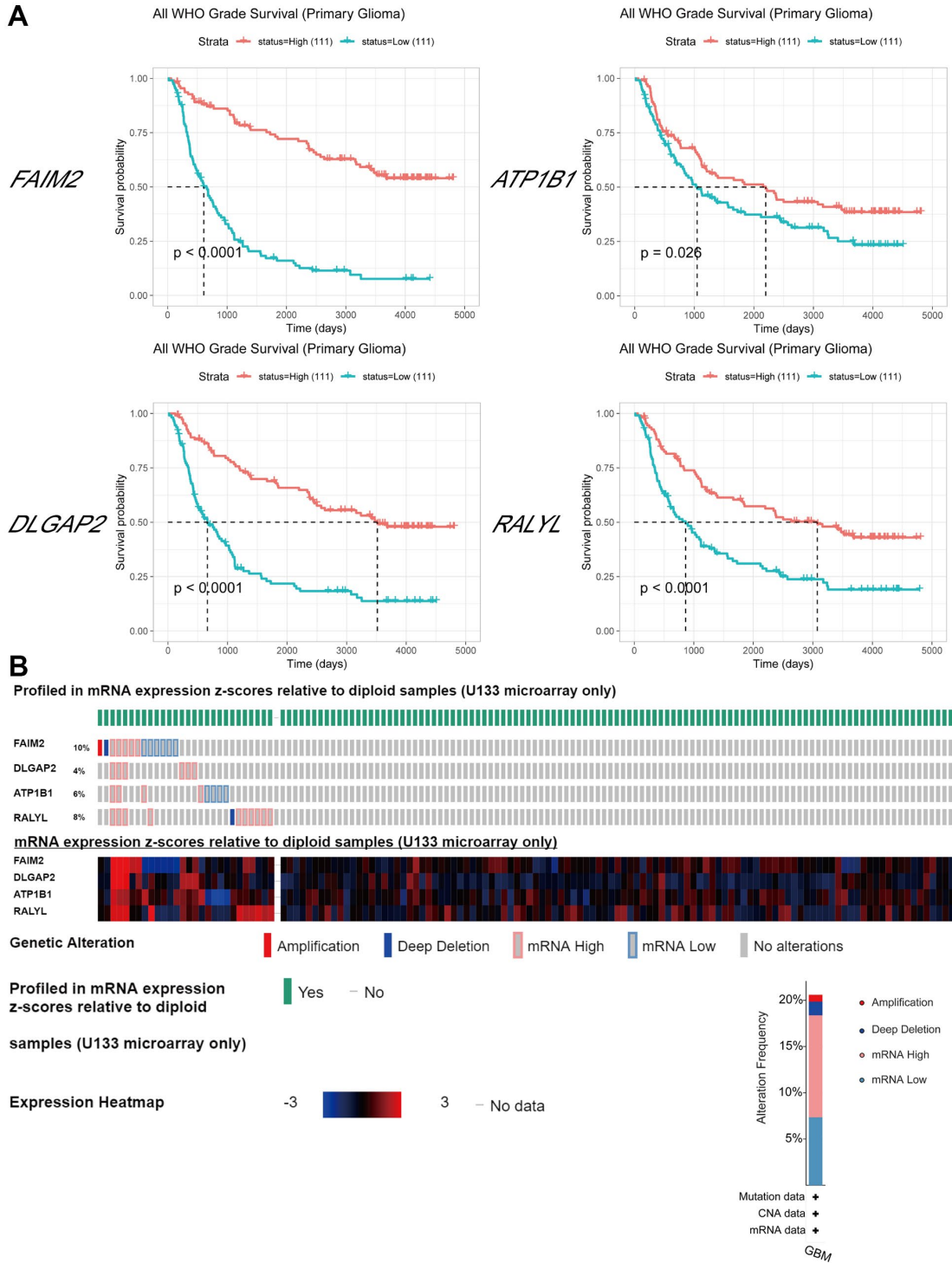
Supplementary Figure 1. Survival analysis and genomic alterations of 4 target mRNAs. (**A**) Survival analysis of 4 target mRNAs by CGGA. (**B**) Summarizes genomic alterations in the 4 queried genes, *FAIM2*, *DLGAP2*, *ATP1B1*, and *RALYL,* across a set of GBM samples by cBioPortal. Each row represents a gene, and each column represents a tumor sample. Red bars represent gene amplifications, and blue bars represent deep deletions.
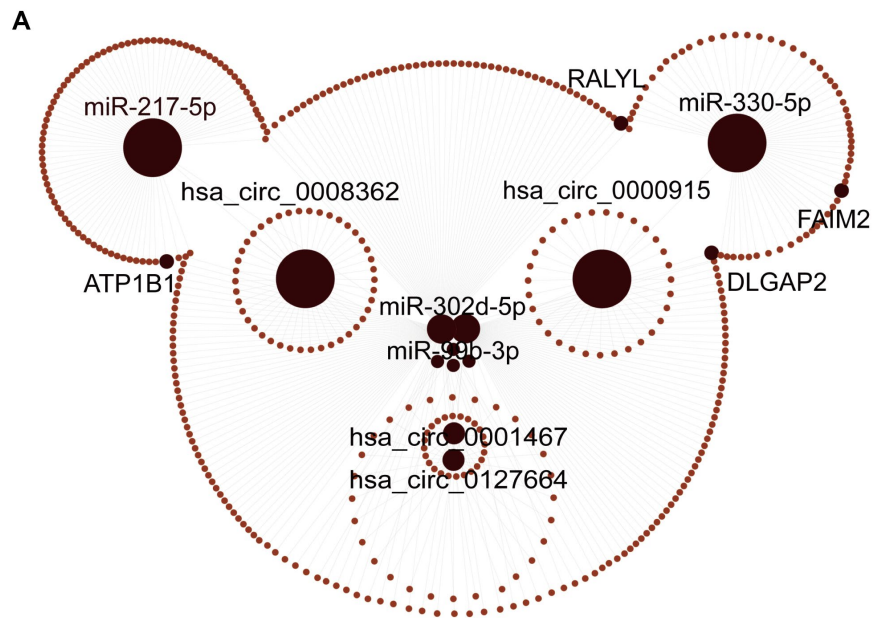
Supplementary Figure 2. CircRNA-miRNA-mRNA network map. (**A**) network predicting target miRNAs of hsa_circ_0000915, hsa_circ_0127664, hsa_circ_0008362, and hsa_circ_0001467 and their top target genes. CircRNAs, target miRNAs and genes are represented by brown nodes. Gray lines indicate a regulatory relationship.
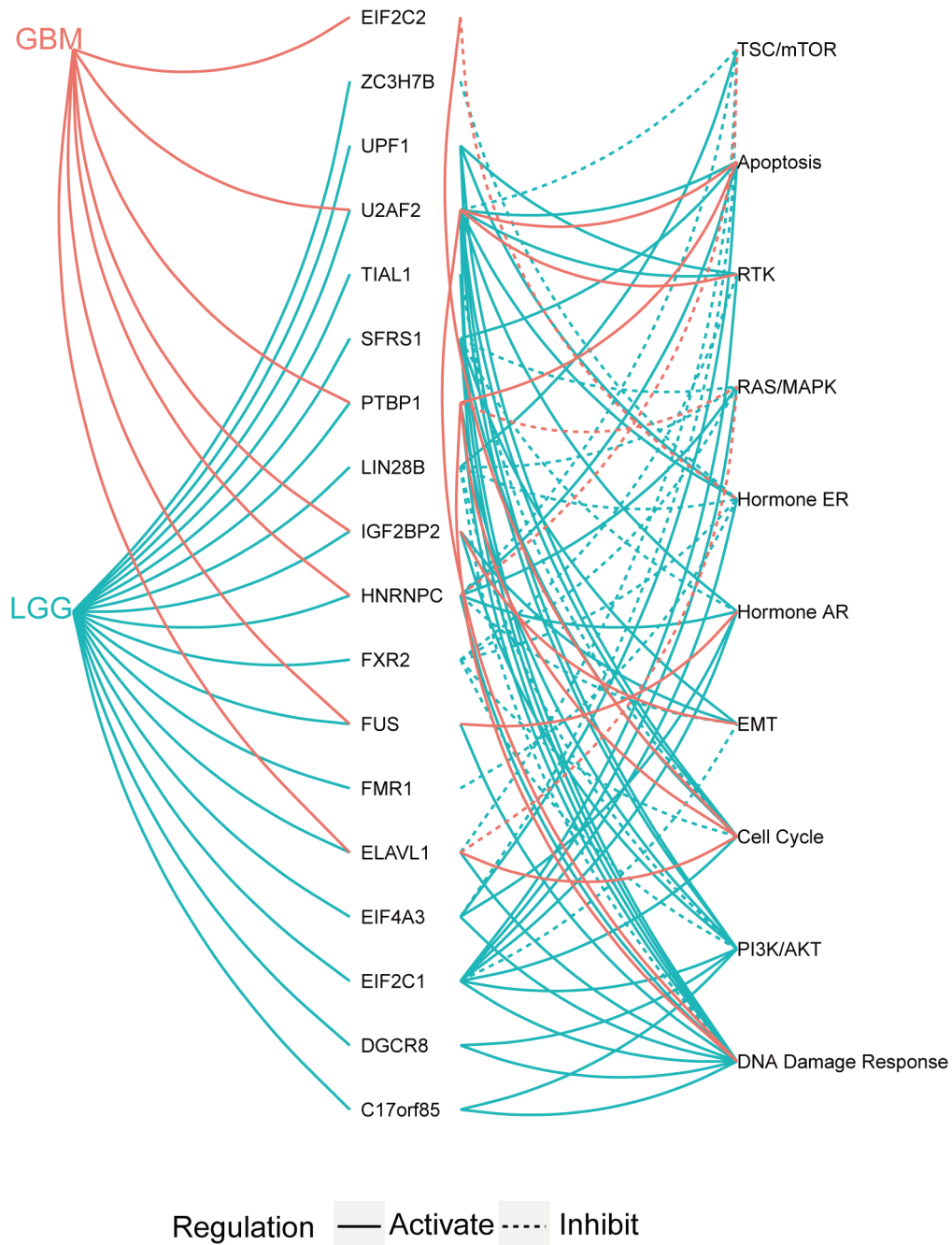
Supplementary Figure 3. Interaction map of RBP genes and activation and inhibition of cancer pathways.

hsa_circ_0127664

hsa_circ_0008362
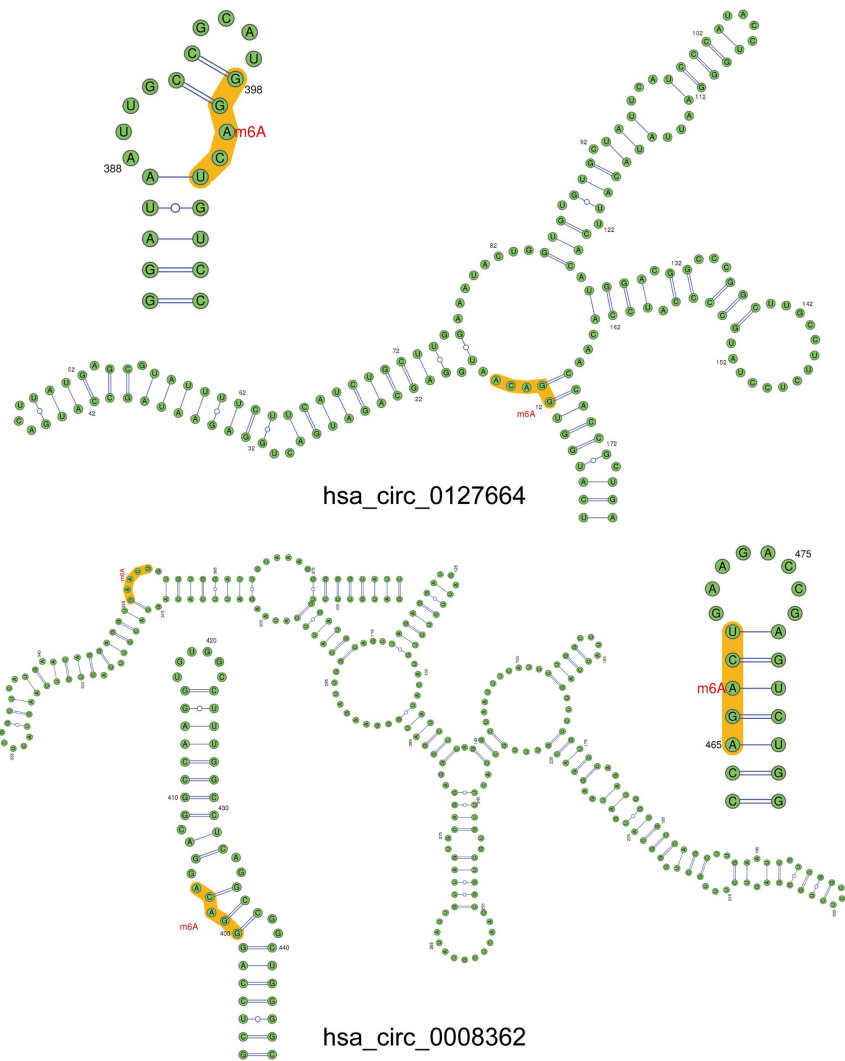
Supplementary Figure 4. Visualization of the local m⁶A site structure of circRNAs.

Supplementary Tables

Please browse Full Text version to see the data of Supplementary Tables 2, 3.

Supplementary Table 1. Primer sequences of candidate circRNAs.

Gene	Forward and reverse primer	Product length (bp)
hsa_circ_0127664	hsa_circ_0127664-F1 CCGAGCTTGTGAAAGTTGTT hsa_circ_0127664-R1 GGCCGTCCATGTGAATGTAT	150
hsa_circ_0008362	hsa_circ_0008362-F1 AGCCCATTACTCAGGATGAC hsa_circ_0008362-R1 TCTGACTGCATCTCCACTTC	115
hsa_circ_0000915	hsa_circ_0000915-F1 CGGCCCCAAGGCAGGGAAC hsa_circ_0000915-R3 CTCCAGCGACGTCTGCAGATGTACG	119
hsa_circ_0001467	hsa_circ_0001467-F2 AGACTTTGATAGTTGCGGTGCTGTT hsa_circ_0001467-R2 ACGGCCAGCAAATACTGCCA	142
GAPDH	GAPDH-F AGAAGGCTGGGGCTCATTTG GAPDH-R GCAGGAGGCATTGCTGATGAT	140

Supplementary Table 2. The 129 potential target miRNAs of the 4 identified circRNAs.

Supplementary Table 3. Information on the circRNA-miRNA-mRNA network.

Supplementary Table 4. Clinical information for relevant patients in RNA-seq.

Patient	Age	Gender	WHO grade
High grade1	65	Female	WHO IV
High grade2	50	Male	WHO III
High grade3	53	Female	WHO IV
High grade4	78	Female	WHO IV
High grade5	36	Female	WHO IV
High grade6	53	Female	WHO IV
Low grade1	53	Male	WHO II
Low grade2	64	Male	WHO I-II
Low grade3	37	Female	WHO II
Low grade4	35	Male	WHO II
Low grade5	32	Female	WHO II
Low grade6	38	Male	WHO II
Normal1	65	Female	
Normal2	53	Female	
Normal3	35	Male	
Normal4	38	Male	
Normal5	36	Female	